

EXAMINING THE INFLUENCE OF LAND USE AND LAND COVER ON RIVER MORPHOLOGY: CASE OF LIKANGALA RIVER, ZOMBA, MALAWI

LONJEZO KAUNDAMA_WQM/017/18

AND

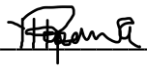
HLAZO PHIRI_WQM/025/19

Dissertation submitted to Ndata School of Climate and Earth Sciences of the Malawi University of Science and Technology in partial fulfilment of the requirements for the Bachelor of Science degree in Water Quality and Management

14TH JUNE, 2024

PROPOSAL APPROVED BY:

SUPERVISOR:

Mr, H. Yapuwa Signature: 

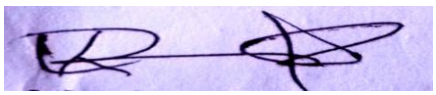
ASSESSOR:

Title, Initials, Name Signature: _____

DECLARATION

We, (KAUNDAMA LONJEZO and PHIRI HLAZO) declare that this research project represents our work and that it has never been submitted to this institution or any other institution for any academic purpose. All sources of information have been appropriately acknowledged.

RESEARCHERS:

Mr. L. Kaundama Signature: 

Mr. H. Phiri Signature: 

DISCLAIMER

This document describes work undertaken as part of a programme of study at Ndata School of Climate and Earth Sciences of the Malawi University of Science and Technology. All views and opinions expressed therein remain the sole responsibility of the authors, and do not necessarily represent those of the school.

COPYRIGHT STATEMENT

This copy of the dissertation has been supplied on condition that anyone who consults it, is understood to recognize that its copyright rests with its authors and that no quotation from the dissertation and no information derived from it may be published without acknowledgement.

ABSTRACT

In the face of escalating environmental challenges, the changes in land use and land cover emerges as a persistent threat, profoundly impacting the stability of natural water systems. This study investigates the influence of land use and land cover (LULC) changes on river morphology, with a particular focus on the effects of urbanization, agriculture, and deforestation. Utilizing satellite imagery for years 1993, 2002, 2013 and 2022, GIS tools and Google Earth Pro, the research examines how different land uses impact river characteristics such as width, length, and sinuosity. Data were collected from different sources including the Earthexplorer.usgs.gov for Landsat images. LULC maps for the years 1993, 2002, 2013 and 2022 were generated incorporating the spectral indicators such as vegetation, water, built up area, bare land and barren land. The findings revealed that built up land from 1993 to 2022 underwent the most significant changes by increasing from 10.87km^2 to 36.02km^2 representing 69.82% followed by bare land which changed from 77.71 km^2 to 109.81km^2 representing 29.23% while vegetation decreased by 30.07 km^2. Water on the other hand changed from 5.33 km^2 to 5.86km^2. The study also employed the analysis of hydro-meteorological data which was obtained from DCCMS and Ministry of Water and Sanitation in the water resources department for rainfall and streamflow data respectively. The results revealed a decreasing trend in both rainfall and streamflow. The river morphology changed as well with average length changing from 20.96 km to 10.56 km, sinuosity decreased from 1.87 to 1.5. The substantial correlations between LULC changes and alterations in river morphology were done. Specifically, urbanization and deforestation as a result of built up and bare land increase to the expense of vegetation, are linked to increased sedimentation and reduced river width, while rainfall revealed a strong relationship with rainfall contributing to significant changes in river sinuosity. These results underscore the importance of sustainable land management practices that consider the impacts on river characteristics and its ecosystems.

ACKNOWLEDGEMENT

First, we would like to express our gratitude to Mr. H. Yapuwa, our supervisor whose expert advice, continuous support, useful suggestions and challenging questions guided us through our study successfully. His insights, patience, and expertise were crucial in shaping our research and ensuring its quality. This gesture cannot be undermined; we really appreciate it.

We are grateful to Mr. Francis Chauluka, MUST Research Coordinator, for his support throughout the entire period of our study. His guidance and encouragement have been instrumental in the successful completion of this project.

We are also grateful to our colleagues and peers who provided feedback and assistance during various stages of this research. Their constructive criticism and suggestions were invaluable in refining our work. Additionally, we would like to acknowledge the resources and facilities provided by the university, which greatly facilitated our research process.

Finally, we extend our heartfelt thanks to our families and friends for their unwavering support, understanding, encouragement and interest into our studies. Their understanding and motivation have been a constant source of strength for us.

TABLE OF CONTENTS

DECLARATION iii
DISCLAIMER iv
COPYRIGHT STATEMENT v
ABSTRACT vi
ACKNOWLEDGEMENT vii
1. INTRODUCTION 1
1.1. Background 1
1.2. Problem Statement 2
1.3. Objectives 3
1.4. Research Questions 3
1.5. Significance of the study 3
1.6. Research Hypothesis (Ha) and null hypothesis (Ho) 4
2. LITERATURE REVIEW 5
2.1. Introduction 5
2.2. Impacts of urbanization on river morphology 5
2.3. Case Studies 7
2.4. Conclusion 9
3. METHODOLOGY 10
3.1. Study area 10
3.2. Research design 11
3.3. Data collection 12
3.4. Methods 13
4. RESULTS AND DISSCUSSIONS 23
4.1. Changes in land use and land cover (LULC) in the Likangala river basin from 1993 to 2022. 23
4.2. Hydro-metrological trends of the Likangala watershed from 1993 to 2022 28
4.3. DISCUSSION 51
5. CONCLUSION 54
6. RECOMMENDATIONS 55
7. REFERENCES 58

ACRONYMS/ABBREVIATIONS

ANN	Artificial Neutral Network
DCCMS	Department of Climate Change and Meteorological Services
DPSIR	Driver-Pressure-State-Impact-Response
GPS	Geographical Positioning System
Ha	Research hypothesis
Ho	Null hypothesis
LULC	Land use and landcover
MLR	Multiple Linear Regression
MOLUSCE	Modules for Land Use Change Evaluation
NWRA	National Water Resources Authority
QGIS	Quantum Geographical Information System
SPOT 5	Satellite Pour l'Observation de la Terre
USGS	United States Geological Survey

LIST OF FIGURES

Figure 1: Map of the study area.....11
Figure 2: Methodology flow diagram..... 12
Figure 3: Spearman's rho test 17
Figure 4: Geographical control points on Likangala River.....22
Figure 5: Map of the study area 26
Figure 6: Post-classification LULC change detection 27
Figure 7: Temporal variations in LULC of Zomba city_1993-2022 27
Figure 8: The annual rainfall trend from 1993 to 2022 32
Figure 9: Rainfall trend for dry season from1993 to 2022 32
Figure 10: Rainfall trend for dry season from 1993 to 2022.....33
Figure 11: The Pettit homogeneity test of the annual rainfall.....34
Figure 12: The Pettit homogeneity test of the dry season.....35
Figure 13: The Pettit homogeneity test of the wet season. 35
Figure 14: Annual streamflow trend from 1993-2022.....39
Figure 15: Wet season streamflow trend from 1993-2022 39
Figure 16: Dry season streamflow trend from 1993-2022 40
Figure 17: The Pettit homogeneity test of the annual streamflow..... 41
Figure 18: The Pettit homogeneity test of the dry season streamflow. 42
Figure 19: The Pettit homogeneity test of the wet season streamflow. 42
Figure 20: Scatter plots showing the annual relationship between rainfall and streamflow in Likangala River 43
Figure 21: Scatter plots showing the wet season relationship between rainfall and streamflow in Likangala River 44
Figure 22: Scatter plots showing the wet season relationship between rainfall and streamflow in Likangala River 45
Figure 23: Map showing change in river length, width and course 48
Figure 24: Scatter plots showing relationship between variables ..... **Error! Bookmark not defined.**

LIST OF TABLES

Table 1: Data used in the study and their sources 14
Table 2: LULC Classification scheme used in the study area 14
Table 3: GPS coordinates for selected sites 21
Table 4: shows details of reference points for each LULC class. 23
Table 5: Land use/land cover changes result depicting area change and annual rate of change for the study periods (1993–2022) 28
Table 6: 1993-2022 Land Cover Change matrix (km2) 28
Table 7: Summary of Mann-Kendall test results of monthly and seasonal Rainfall data from 1993-2022 29
Table 8: Sen's Slope test results for monthly, annual and seasonal rainfall from 1993-2022 30
Table 9: Summary of Mean, Std. deviation and Coefficient Variation % for Rainfall data from 1993-2022 31
Table 10: Summary of Mann-Kendall test results of monthly and seasonal streamflow data from 1993-2022 36
Table 11: Sen's Slope test results for monthly, annual and seasonal streamflow from 1993-2022 37
Table 12: Summary of Mean, Std. Deviation, coefficient Variance % 38
Table 13: Correlation matrix showing significant insights into how variables interact and influence one another in the study area. 50

1. INTRODUCTION

1.1. Background

The response of river morphology to watershed alteration is an important body of research in which rivers have historically been underrepresented (Owen, 2020). These alterations are a result of land use due to population growth that has triggered urbanization which involves the transition of areas from rural to urban, resulting in the growth and expansion of cities and towns (Henderson, 2005). As urban areas develop, they undergo significant changes in land use and infrastructures, these surfaces replace natural landscapes like soil and vegetation (Abernethy & Rutherfurd, 2014). Although numerous studies have linked anthropogenic alterations of landcover with channel widening (Julian, 2012), others found that the dominant response of some channels is a reduction of the channel width and depth (Fausstini, 2009; Bartley, 2008 & McGranahan, et al., 2015). This phenomenon has sparked growing interest in understanding the influence of land use and land cover on hydrological cycles, stream morphology, and stream flow rate (McCann, 2013). The accumulation of impervious surfaces in urban areas can significantly impact the local hydrograph, which is a graphical representation of the flow of water in a river or stream over time (Bonta, et al., 2015), often exhibits rapid runoff and increased peak flow, leading to localized flooding. This process often triggers alterations in river forms, such as the narrowing and deepening of channels, the loss of natural meanders, and the removal of vegetation along riverbanks which leads to disruption of natural habitats for aquatic species (Chithra, et al., 2015; Chithra, et al., 2015 & Zhang, et al., 2023). Land use and land cover does not only lead to infrastructure development, it has also led to an increase in agricultural land (De Marco, et al., 2020). In the study on Canadian rivers, Julian et al. (2012) found that as land on the banks of the river was converted to agricultural use, the banks became more susceptible to erosion. An increased erosion from croplands caused an increase in active channel area, eventually causing a decrease in available cropland. As cited in Owen, (2020), IPBES, (2019) found that of all the various methods by which humans alter their environment, change in land cover has the largest global impact.

Therefore, understanding the influence of land cover and land use from urbanization on river morphology with a focus on width, valley length, sinuosity, and bank shifting is crucial for sustainable urban planning and environmental management. Proper management of impervious surfaces and the hydrograph is essential to mitigate the negative impacts of land use and land cover on aquatic ecosystems and water quality.

1.2. Problem Statement

A river basin, a distinct hydrological unit has its own 'geo-bio-cultural' interactions (Chakrabarti, 2018). Any change in the water-sediment regime within a watershed, triggered by either natural or anthropogenic causes has a lagged effect on the downstream activities of the river in terms of morphology as well as lateral banking stability. Rivers provide readily available water for numerous uses in rural, peri-urban, and urban areas apart from the provision of other numerous ecosystem services such as groundwater recharge and, provision of habitats to aquatic life (Mweta & Changadeya, 2022).

The Likangala River is a significant waterway in the southern part of Malawi that empty its water into Lake Chilwa (Pullanikkatil, et al., 2016) which is the second largest lake in Malawi according to Jamu, et al., (2010). These water bodies serve as critical habitats for fish and wildlife, sustaining important fish populations that provide a source of livelihood for local fishing communities and contribute to the region's food security. The Likangala Rice Irrigation Scheme, which harnesses the waters of the Likangala River, significantly benefits from the river by using its waters to irrigate agricultural fields, enhancing crop yields and year-round farming. Therefore, it is important to note that any change in the Likangala River watershed has a direct impact on the Likangala River, Likangala irrigation scheme, and Lake Chilwa and its ecosystems. This has been witnessed in the siltation of Lake Chilwa as a result of deforestation and the conversion of agriculture and forest land to homestead development (Jamu, Chimphamba, & Brummett, 2010). A study by Makwinja, et al., (2014) established that deep pools in the Likangala River became shallower due to increased silt deposition from the upper part of the catchment. Another study by Pullanikkatil, et al., (2016) which employed remote sensing and the DPSIR approach to evaluate land use change in the catchment area of the Likangala River, revealed that land use changes have caused a decline in vegetation cover and an upswing in built-up areas. These transformations can bring about increased runoff, erosion, and sedimentation, which can adversely affect river morphology. This argument is supported by a study done by De Marco, et al., (2020) who found that urbanization can precipitate a shift in land use, heightened pollution, and variations in runoff patterns, all of which can significantly influence river systems, including alterations in hydrology, and morphology.

It is therefore indispensable to research the influence of land use and land cover on river morphology with a focus on its sinuosity, width, length, bank shifting over time.

1.3. Objectives

To examine the influence of Land use and land cover on river morphology of Likangala river with respect to sinuosity from 1993 to 2022.

1.3.1. Specific Objectives

i. To assess the changes in land use and land cover (LULC) in the Likangala river basin from 1993 to 2022.
ii. To assess the hydro-metrological trends of the Likangala watershed from 1993 to 2022.
iii. To establish the relationship between land use and land cover (LULC) changes, hydro-meteorological trends, and river morphology variations in the Likangala river from 1993 to 2022.

1.4. Research Questions

i. What have been the trends in land modification within the Likangala watershed over the past three decades?
ii. What have been the patterns of rainfall and discharge in the Likangala watershed over the last three decades?
iii. What are the observed morphological changes in the Likangala River for the past three decades?

1.5. Significance of the study

To plan a sustainable urban environment, one must comprehend how land use with reference to infrastructure development, and agriculture affects water systems and grasp the importance of river morphology for developing predictive models essential in water resource management and flood risk mitigation to protect people and property.

The research provides new insights into how the Likangala River's hydrology and morphology have changed over time, and how these changes are influenced by land use and land cover and other factors. Understanding this is essential for managing the river's resources sustainably.

Therefore, policymakers, urban planners, and environmentalists may use the study's insights to create practical mitigation plans for the adverse effects of land use and land cover on river ecosystems.

1.6. Research Hypothesis (Ha) and null hypothesis (Ho)

The research hypothesis is that the Likangala River has experienced significant morphological changes over the past three decades due to land use change. The null hypothesis is that there have been no significant morphological changes in the Likangala River over the past three decades due to land use change.

2. LITERATURE REVIEW

2.1. Introduction

Land use and land cover coupled with urbanization is a major global trend that is having a significant impact on river morphology (Zhou & Chen, 2018). As cities grow, they encroach on riverine ecosystems, leading to changes in land use, vegetation cover, and impervious surfaces. This is supported by (Abate, et al., 2015) who found that changes land use land cover changes have a profound impact on river channel morphology, including changes in width, depth, sinuosity, and bedload transport.

2.2. Impacts of urbanization on river morphology

There is a growing body of literature on the interactions between urbanization and river morphology. A review of this literature by Ahiablame et al. (2019) identified several key impacts of urbanization on river morphology, including increased river channel width, decreased river channel depth, reduced river channel sinuosity, increased bedload transport, and increased flooding. These impacts are caused by a variety of factors, including, increased impervious surfaces such as roads and buildings which prevent rainwater from infiltrating into the ground and instead cause it to run off into rivers (Yao, Wei, & Chen, 2016).

2.2.1. Impervious surfaces

With the same drainage condition, different impervious distribution within the catchment may alter the final runoff hydrograph at the catchment outlet, particularly for peak discharge (Meierdiercks et al., 2010). Guan et al. (2015), who observed that the changes in imperviousness with various development options in small catchments result in considerable flow variations, came to a similar conclusion. Therefore, providing more scientific direction for landscape/imperviousness designs in urban settings may aid in urban flood control by establishing a quantifiable link between imperviousness and rainfall-runoff at finer sizes, such as a neighbourhood, parcel, or even smaller area. However, in big urban watersheds, landscape patches are always larger and more complex than in small catchments, which leads to distinct runoff flows and trip durations (Walsh et al., 2009, Yang et al., 2011).

2.2.2. Riparian vegetation

Riparian vegetation helps to stabilize riverbanks and reduce erosion. Riparian and in-channel vegetation can reduce stream erosion rates but it is unrealistic to expect

revegetation to eliminate all erosion. By accepting some channel change as inevitable, a managed riparian zone provides space within which river form and processes can be allowed to adjust. Urbanization has accelerated the natural and essential processes of river channel adjustment, often to unacceptable levels, which can make rivers more susceptible to erosion and channel widening (Abernethy & Rutherfurd, 2014 & Singh, Tiwari, & Singh, 2021).

2.2.3. River channel straightening

River channel straightening is a common practice used in urban areas to accommodate urban development, which requires alterations to the natural meandering patterns of rivers (Kwamboka, 2014). Through channelization, embankment building, or excavation, this process simultaneously increases water flow velocity and decreases the sinuosity of river channels. Decreased sinuosity results in faster water flow, which amplifies erosive forces and raises sediment transport and bed scouring rates (Yousefi, et al., 2018). Consequently, this results in increased vulnerability to erosion, ultimately contributing to channel widening. The interplay between reduced sinuosity, enhanced water flow velocity and intensified erosive processes leads to a continuous process of channel enlargement, representing a dynamic equilibrium between erosion and sediment deposition within the river system (Kamarudin, et al., 2014).

2.2.4. Increased bedload transport

Increased runoff and erosion can lead to increased bedload transport. This can lead to the deposition of sediment in the downstream reaches of rivers, which can increase the risk of flooding (Zhang, et al., 2023). Sediment not only changes the shape of rivers but also carries many pollutants. Increases in sediment deposition have negative impacts on the basin environment, increasing flood hazards and shortening the lifespans of infrastructure (Vercruysse, et al., 2017). Therefore, it is necessary to clarify the trend and driving forces of sediment load variation. It is generally believed that climate changes and human activities contribute to local decreases or increases in sediment load in different river basins. For example, the increasing sediment load in High Mountain Asia mainly is the result of accelerated thermally driven glacier-permafrost melt and increased precipitation (Li, et al., 2021). However, other studies have found that the sediment load was significantly reduced in most Asian rivers because of accelerated human disturbance including dam construction and vegetation restoration (Walling, 2011; Wang, et al., 2015; Yang et al., 2018; Li et al., 2020 & Peng et al., 2020).

2.3. Case Studies

2.3.1. Texas-USA

The study by Owen, (2020), examined the impact of urbanization on the morphology of the Brazos, Colorado, and Trinity rivers in Texas. The study found that the average maximum sediment size in the Brazos River decreased from 242 μm to 193 μm, with a steady decline from sampling sites upstream of Waco to locations downstream of Waco city. The average maximum sediment size in the Trinity River grew from 153-271 μm, indicating a shift from fine sand to medium sand. This suggests that urbanization may lead to morphologically stable river channels with reduced biological variety. However, the study found that for small catchment areas, land cover of the immediate sub-watershed does not have a discernible effect on sediment size or discharge. Owen suggested that a more complete study should also assess meteorological data for the city centres and surrounding areas to determine possible effects of urbanization on river morphology

2.3.2. China

Deng, et al., (2015) examined the temporal and geographical change of river system geomorphology in the Taihu Region during the past 50 years in connection with urbanization. The study was based on data generated from topographic maps and remote sensing photos. The findings showed a sharp decline in the number of river systems, a shift in the shape of river channels toward bigger, straighter ones, and a tendency toward simplification of the network structure. While the decrease in river sinuosity during the slow urbanization period was more severe, the changes in river density, water surface ratio, river development coefficient, main river area length ratio, and box dimension during the rapid urbanization period were significantly greater than those during the slow urbanization period. Conversely, the low-urbanized regions saw the most dramatic changes in river indicators, and the spatial disparities in changes in the river development coefficient were the highest. Furthermore, the strongest correlations were found between population urbanization and changes in river systems, and the changes in the water surface ratio and urbanization. The study makes clear how urbanization affects waterways.

2.3.3. Kaduna State, Nigeria

The research by Butu et al., (2020) looked into modifications to the River Kaduna's channel planforms. Sentinel-2 and SPOT 5 satellite mosaics were used to enhance topographic maps. The findings demonstrated that there were notable variations in channel width, braiding, migration, and sinuosity index in addition to channel length. Reduced velocity and Stream

Energy, the kind of sediment being transported, the silt materials being transported in suspension, and the movement of coarse sand and gravel by lift and drag processes which are easily deposited and cause the channel to contract and braid were all clear indicators of these changes. With no signs of lateral abrasion, the channel migrated gradually as it shifted in bends. The sinuosity index was not considerably impacted by changes in channel length either. The fact that the channel was comparatively stable and that there was minimal lateral abrasion was another finding in favour of the hypothesis that the materials being moved and deposited came from the watershed. The observed modification in the waterway was mostly caused by anthropogenic influences, including deforestation, urbanization, and agricultural activity. The researchers proposed that to overcome this problem, it is necessary to promote the mining of sand and gravel from braided channels to provide sinks for sediments that would otherwise be deposited downstream. Canopies for exposed surfaces and a decrease in the amount of silt available required the catchment region to be forested.

2.3.4. Lilongwe Malawi

In the study, (Kapatamoyo, Katonda , Chauluka, & Gondwe, 2023) employed Remote Sensing and GIS to detect and analyse LULC change for the years 1998, 2008 and 2018 in Lilongwe city. The maximum likelihood algorithm was adopted for supervised classification Landsat TM and Landsat OLI images. Classification results showed that built up area increased substantially whereas bare land and vegetation declined, while water remained constant throughout the study period. Post classification comparison of the classified images based on the transition matrix revealed that for the period of 1998 to 2008, vegetation had the highest transition with 47.35 km2 (47.20%) of its total area in 1998, the majority being converted to bare land (40.24 km2), built up area (7.05 km2) and water (0.056 km2). The results further showed that built up area increased at an annual rate of 7.8%, 14.5% and 16.81% for the period of 1998 to 2008, 2008 to 2018 and 1998 to 2018 respectively. The overall accuracies for 1998, 2008 and 2018 images were 95.46%, 94.23% and 89.73% respectively. In a nutshell, the study unveiled LULC change dynamics for Lilongwe city and the rate at which changes were taking place. With an ever-increasing urbanization in this city, these findings present a call for the city to strengthen measures for restoring the deteriorated environment in order to ensure a sustainable environment for all city dwellers.

2.4. Conclusion

For sustainable urban planning and environmental management, it is crucial to comprehend the intricate link between urbanization and river morphology. To lessen urbanization's detrimental effects on river systems, impermeable surfaces and the hydrograph must be managed properly. Understanding how urbanization affects river morphology can help us safeguard the resilience and ecological integrity of riverine ecosystems while advancing sustainable urban growth. This study attempts to examine more closely how land use changes brought about by urbanization have impacted the lower portions of the Likangala River system's channel platforms. It also analyses the changes that have occurred in the river watershed during the previous three decades.

3. METHODOLOGY

3.1. Study area

The Likangala River, 15°22′-15°30′ S, 35°15′-35°37′ E, at 631 m to 1 603 m above sea level and with a catchment area of 756 km is about 50 km long (Chidya et al. 2011). The Likangala catchment is affected by increasing population which has resulted in urban sprawl with many new settlements in Zomba city and Thondwe town, the two major urban areas in Zomba District (Pullanikkatil, Palamuleni, & Ruhiiga, 2016). The according to (Pullanikkatil, Palamuleni, & Ruhiiga, 2016), Likangala catchment is 756 km^2. And has several rivers including Mulunguzi which forms its sub catchments. However, this study combined sub catchents for rivers that flow through the city and empty its water into Likangala before Mkokangowo gauging site. The area of this sub catchment is found to be 232.15km^2. The river is perennial, with a large difference in water discharge over the year, with a peak in wet season, which normally occurs around November until April. The rainfall distribution is fairly uniform and the climate is a tropical wet and dry or dry savanna. The study area contains a variety of land uses which include forest, residential, commercial and agriculture areas. Increased human activity has attributed to 6.59% population growth rate of Zomba city annually, which led to the population growing from 65,915 to 116,797 between 1998 and 2022 alone (National Statistical Office, 2023; Strachan et al., 2021, (UNIMA, 2024)

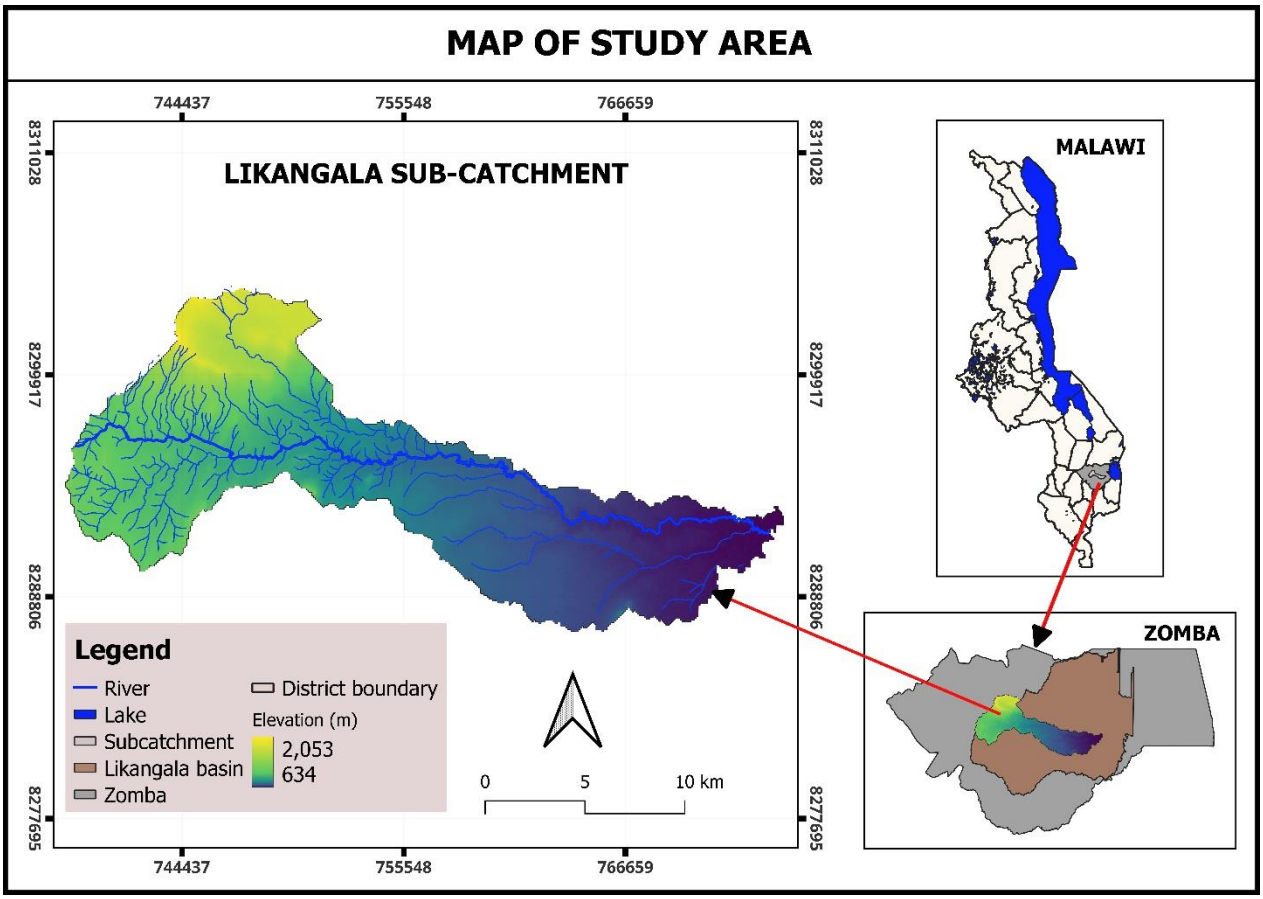


Figure 1: Map of the study area

3.2. Research design

This research is quantitative research which involved collecting and analysing numerical data to answer research questions or test hypotheses. It focused on obtaining quantifiable and measurable data to draw conclusions and make inferences about urbanization hydrological characteristics and Likangala River morphological changes.

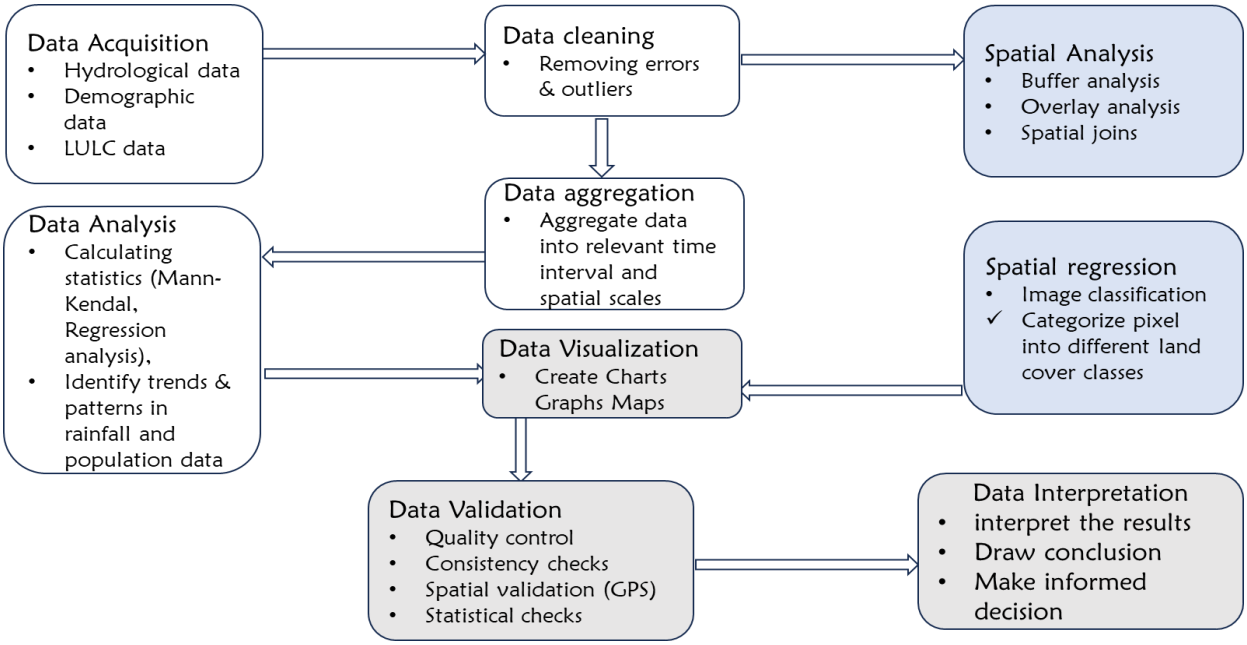


Figure 2: Methodology flow diagram

3.3. Data collection

The data used in the present study consists of the rainfall for 3 meteorological stations Chancellor college (-15.38S, 35.35N) at elevation of 886m, Mulunguzi-20208 (-15.21S, 35.18N) at elevation of 980m and Zomba RTC (-15.40S, 35.69N) at elevation of 900m and streamflow for Mkokangowo gauging site (-15.41S, 35.44N) at elevation of 720m. Both rainfall and streamflow data cover a span of 30 years (3 decades) from 1993 to 2022. The rainfall data was obtained from the MDCCS while the stream flow data was obtained from the department of water resources in the Ministry of Water and Sanitation. The study also employed the GIS and Remote Sensing where Landsat 4-5 TM images from 1993 to 2002 and Landsat 8 OLI from 2013 to 2022 were downloaded at a resolution of 30m x 30m from USGS Web Site path 167/71 and analysed in QGIS software. The Google Earth pro was also used to during ground truth analysis, online reconnaissance survey and river channel characteristics assessment.

3.4. Methods

3.4.1. Determining the land use change in the Likangala River catchment over the past three decades.

LULC Detection

Land use and land cover (LULC) change are one of the indicators for the urbanization process for it is influenced by human activities on landscape (Lui, et al., 2020 & Felix & Hidayati, 2022). The simulation model helps to know the transition of changes in the past to the present, to find out the transition patterns, and to generate predictions in the future from the detected transition patterns.

This study involved the collection of land use data of the area from 1993 to 2022. Landsat 5 Thematic Mapper (TM), and Landsat 8 Operational Land Imager (OLI) satellite imagery from Path 168/Row 71 with a 30 m spatial resolution and a 16-day repeat cycle was obtained from the USGS. The study also used other data type which have been summarised in table 2. The coordinate system of all dataset was uniformly set to EPSG:32736 WGS/84 UTM Zone 36S.

Images downloaded ranged from September to December because during this period the skies were almost clear. Using the Semi-Automatic Classification Tool, the pre-processed dataset was clipped to the extent of the study area. The composite images were created from a selection of visible bands from the clipped data sets to aid the process of classification. Particularly, the false colour composites were created using spectral bands 3, 2 and 1 for Landsat 5 TM and 5, 4, 3 for Landsat 8 OLI. Land use data was classified into vegetation, water, built up area, bare land and barren land. These classes with their associated descriptions were adopted from (Manyungwa, 2023) (Felix & Hidayati, 2022) (Jamu, Chimphamba, & Brummett, 2010) (Kapatamoyo, Katonda , Chauluka, & Gondwe, 2023); (Badapalli, Kottala, Rajasekhar, & Ramachandra, 2018); (Marondedze & Schutt, 2019); (Mawenda, Watanabe, & Avtar, 2020).

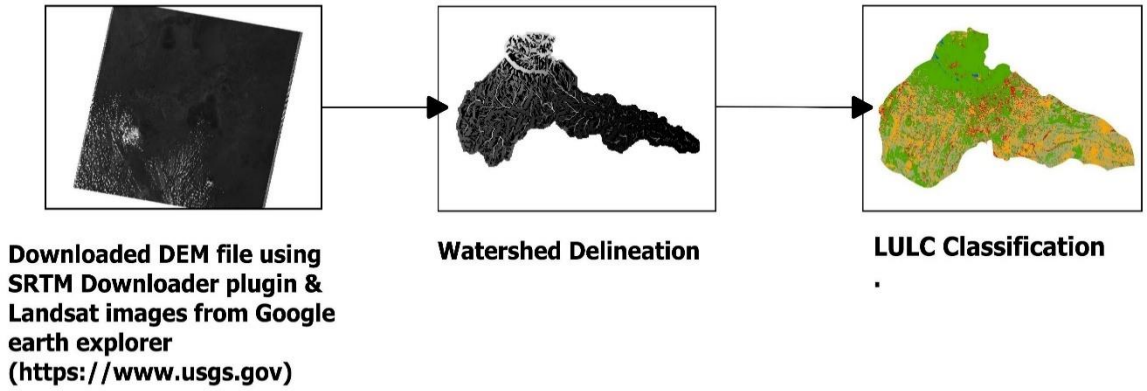


Figure 3: Processes involved in LULC change analysis

Table 1: Data used in the study and their sources

Data type	Collection date	Data source
Landsat 05 Satellite imagery	1993-10-16	USGS
Landsat 05 Satellite imagery	2002-09-01	USGS
Landsat 08 Satellite imagery	2012-11-03	USGS
Landsat 08 Satellite imagery	2022-09-17	USGS
DEM file	N/A	NASA (EOSDIS)
Rainfall data	1993-2022	DCCMS
Hydrological data	1993-2022	Water Resources Department, Ministry of Water and Sanitation
River path	2007-2022	Google Earth Pro

Table 2: LULC Classification scheme used in the study area

LULC Class	Description
Vegetation	Forest on customary land, deciduous forest
Water	Areas covered with water
Built up Area	Residential, commercial and services, industrial, and transport
Bare land	Areas with no, rocky or landfill sites
Barren land	Areas with spacey vegetation, abandoned farms and cultivated areas

3.4.2. Assessment the hydro-metrological trends of the Likangala watershed from 1993 to 2022

The data has been divided into two periods, wet and dry seasons. The hydrological period (wet) in Malawi starts in November and ends in April while the dry season start in May and ends in October (Kapatamoyo, Katonda , Chauluka, & Gondwe, 2023).

3.4.2.1.Missing data

In addressing the issue of missing rainfall and streamflow data, multiple imputation (MI) method was performed in SPSS to ensure that the robustness and reliability of our analysis. The MI was chosen for its ability to handle missing data by creating multiple complete datasets and accounting for the uncertainty inherent in imputing missing values (Noor, 2013) (Chen, Xu, Wang, & Shen, 2019). Multiple imputations have gained popularity as an effective technique for handling missing data in recent years, surpassing alternative methods in predicting missing rainfall values, as evidenced by the studies of (Sattari, Rezazadeh, & Kusiak, 2017) (Miro, Caselles, & Estrela, 2017) (Jakhar, Mishar, & Poonia, 2018) (Milo, Ekonomi, Margo, & Donefski, 2019). The missing data in the time series for rainfall were observed less than 1% while for the streamflow was observed less than 15%. The following is the mathematical equation for calculating missing data.

Equation 1: Overall Estimate

$$Qm = \frac{1}{m}\sum_{j=1}^{m} Ui$$

Equation 2: Within Imputation Variance

$$Um = \frac{1}{m}\sum_{j=1}^{m} Uj$$

Equation 3: Between Imputation Variance

$$Bm = \frac{1}{m-1}\sum_{j=1}^{m} (Q^j - Qm)^2$$

Equation 4: Total Variance

$$Tm = Um + \left(1 + \frac{1}{m}\right) Bm$$

Equation 5: Degrees of freedom for t-Distribution

$$Vm = (m-1)(1+\frac{Um}{\left(1+\frac{1}{m}\right)Bm})^2$$

Where Qm is the pooled estimate of the parameter of interest, calculated as the average of the estimates from each imputed, Um is the average within-imputation variance, representing the uncertainty within each imputed dataset, Bm is the between-imputation variance, representing the variability between the different imputed datasets, Tm is the total variance, which accounts for both within-imputation and between-imputation variances and Vm is the degrees of freedom for the t-distribution, used for constructing confidence intervals and hypothesis tests.

3.4.2.2. Mann Kendall Test

Using excel-stat the rank based non-parametric Mann-Kendall method was applied to the long-term data in this study to detect statistically significant trends. In this test, the null hypothesis (H_o) was that there has been no trend in rainfall and streamflow over time; the alternate hypothesis (H_1) was that there has been a trend (increasing or decreasing) over time (Adam, et al., 2021). This method was used to analyse the historical hydro-meteorological data in Kasese District in Uganda (Adam, Shire, Ayanle, & Salaheldin, 2021) (Gibson, et al., 2022).

The mathematical equations for calculating Mann-Kendall Statistics, S, V(S) and standardized test statistic Z are as follows:

Equation 6: Statistic test

$$S = \sum_{i=1}^{n-1} \sum_{j=i+1}^{n} sig(Xj - Xi)$$

Equation 7: Means estimator

$$sign(Xj - Xi) = \begin{cases} +1\ if\ (Xj - Xi) > 0 \\ 0\ if\ (Xj - Xi) = 0 \\ -1\ if\ (Xj - Xi) < 0, \end{cases}$$

Equation 8: Variance

$$V(S) = \frac{1}{18}[n(n-1)(2n+5) - \sum_{p-1}^{q} tp(tp-1)(2tp+5)]$$

Equation 9: Standardized test statistic

$$Z = \begin{cases} \frac{S-1}{\sqrt{VAR(S)}} & if\ S > 0 \\ 0 & if\ S = 0 \\ \frac{S+1}{\sqrt{VAR(S)}} & if\ S < 0 \end{cases}$$

In these equations, Xi and Xj are the series observations in chronological order, n is the length of time series, tp is the number of ties for pth value, and q is the number of values. Positive Z values indicate an upward trend in the hydrologic time series; negative Z values indicate a negative trend. If $|Z| > Z_{1-\alpha/2}$, (Ho) is rejected and a statistically significant trend exists in the hydrologic time series. The critical value of $Z_{1-\alpha/2}$ for a p value of 0.05 from the standard normal table is 1.96.

3.4.2.3. Spearman's rho Test.

Spearman's rho test is another rank based nonparametric method used for trend analysis and was applied as a comparison with the Mann-Kendall test. The test which assumes that time series data are independent and identically distributed, the null hypothesis (H_o) again indicates no trend over time; the alternate hypothesis (H_1) is that a trend exists and that data increase or decrease with i. the test statistics R_{sp} and standardized statistics Z_{sp} are defined as

Figure 4: Spearman's rho test

$$Rsp = 1 - \frac{6\sum_{i=1}^{n}(Di - i)\text{^}2}{n(n\text{^}2 - 1)}$$

$$Zsp = Rsp\sqrt{\frac{n-2}{1 - Rsp\text{^}2}}$$

In these equations, Di is the rank of the ith observation, I is the chronological order number, n is the total length of the time series data and Zsp is rainfall/streamflow's distribution table is defined as $t_{(n-2,1-\alpha/2)}$. If $|Zsp| > t_{(n-2,1-\alpha/2)}$, (Ho) is rejected and a significant trend exists in the

hydrologic time series (Ahmad, Tag, Wang, Wang, & Wagan, 2014). A positive value of 'S' indicates increasing trend, where as a negative value indicates a decreasing trend (Chauluka, Singh, & Kumar, 2020); (Kumar, Sigh, Randhawa, Sigh, & Rana, 2014).

3.4.2.4. Sen's slope estimator

This is a non-parametric test widely used for calculating the magnitude of the trend in hydro-meteorological time series (Chauluka, Singh, & Kumar, 2020). Sen's slope is considered better to detect the linear relationship as it is not affected by the outliers in the data (Ray, Das, Mishra, & Al Khatib, 2021) Sen's slope in this study is being applied to calculate the magnitude of the trend for rainfall and streamflow data.

The following equation is used to estimate each individual slope (Qi)

Equation 10: Slope estimator (Qi)

$$Qi = \frac{Xi - Xk}{j - k} \; for \; i = 1, 2, 3, \ldots N$$

Where Xj and Xk are data values at time j and k (j<k). the median of these N values of Ti is sen's estimator of slope which is calculated as

Equation 11: Median of N values

$$Qij \begin{cases} \dfrac{Xi - Xk}{j - 1} & if \; n \; is \; odd \\ \dfrac{1}{2}(Q\dfrac{N}{2} + Q\left[\dfrac{N+2}{2}\right] & if \; n \; is \; even \end{cases}$$

A positive Qi value indicates an increasing trend while a negative value indicates a decreasing trend value in the rainfall and streamflow data series. The unit of Sen's slope is the slope magnitude per year (Ray, Das, Mishra, & Al Khatib, 2021) (Han, Fikiru, & Samerawit, 2023)

3.4.2.5. Pearson correlation coefficient

Cited in (Ali, Hussain, & Faisal, 2019) and (Chauluka, Singh, & Kumar, 2020) states that a widely used Pearson correlation coefficient (r) test statistic measures the degrees of relationships between two continuous variables. It can be computed using the following equation

Equation 12: Pearson correlation coefficient

$$r = \frac{N\sum xy - (\sum x \sum y}{\sqrt{N\sum x^2 - \left(\sum x^2\right).(N\sum y^2 - (y^2)}}$$

Where x and y represent the values of the variables and N represents the total number of elements under study. The range of r lies between -1 to 1. Positive values close to 1 indicate strong correlation between the two variables, while negative values show thr inverse relationship.

Pettitt test

The Pettitt test is a rank based non-parametric statistical test used to detect change points present in data series (Pettitt, 1979). Consider a sequence of random variables X_1, X_2, ..., X_T with change point at time τ, which is divided in two sets with distinct distributions functions: $F_1(X_t)$, t=1, 2, …,τ and $F_2(X_t)$, t= τ + 1, …T.

$$\begin{cases} Ho: F1\ (X) = F2(X)\ (no\ change\ point) \\ H1: F1\ (X) \neq F2(X)\ (change\ point) \end{cases}$$

To detect the change point, the test uses the statistics $U_{t,T}$, similar to the Mann-Whitney test statics for two samples given by (Pettitt, 1979);

$$Ut, T = \sum_{i=1}^{t} \sum_{j=t+1}^{T} sign(Xi - Xj), 1 \leq t < T$$

Where;

$$\begin{cases} 1, if\ X > 0 \\ 0, if\ X = 0 \\ -1, if\ X < 0 \end{cases}$$

The most probable change τ, will be the one that satisfies the following equation;

$$K\tau = U_{t,T} = \max\left|U_{t,T}\right|, 1 \leq t < T$$

Based on asymptotic argument about a test statistic, (Pettitt, 1979) defines the following approximately p-value of the test;

$$P \approx 2Exp(\frac{-6K_{\tau}^{2}}{T^{3}+T^{2}})$$

Thus, given a significance level α, if p< α the null hypothesis, H_0 that the two distributions are equal is rejected.

3.4.3. To assess the relationship between land use and land cover (LULC) changes, hydro-meteorological trends, and river morphology variations in the Likangala river from 1993 to 2022.

River width, length, path and sinuosity of Likangala river, during the assessment was established and analysed in the following ways;

3.4.3.1. River course change detection:

The study employed remote sensing in mapping the course of Likangala river from the year 2007 to 2022. This method has been used by many researcher to assess the channel sifting caused by urbanization and environmental changes (Maurya & Yadav, 2016), (Aung & Tint, 2019), (Yang, et al., 2015), (Madake, Rahate, Khairnar, & Belgamwar, 2024). Google Earth Pro was used to visualize the change of channel pattern so as to identify and measure the changes that has taken place in the status between these periods. The area of interest was identified using the search bar or navigation tools. Historical imagery was used to track changes over time from 2007 to 2022. A polygon was created along the suspected river banks, and elevation changes were analysed using 3D view and terrain features. The path was saved in an KML format. The files were then loaded in QGIS where they were overlayed and saved as shapefiles for map production. During this tour, six suitable locations along the river were purposefully selected, for assessment of river width, length and path shifting. The coordinates for the selected sites are presented in the **table 3** below. The mean channel width and length of the river for the past 15 years was calculated. A linear regression analysis on the mean channel width data was performed in excel stat to identify any significant trends over time.

Length of the river valley in the study section was also measured for calculating Sinuosity index to differentiate sinuous from meandering (Maurya & Yadav, 2016). Rivers having a sinuosity of 1.5 or greater refers meandering, below 1.5 sinuous and straight when sinuosity is below 1.05 (Maurya & Yadav, 2016).

Sinuosity Index was calculated using the following formula.

$$Sinuosity\ Index = (Stream\ Length).(Valley\ length^{-1})$$

$$SI = (Lcmax).(LP^{-1}) = (CD).(XY^{-1})$$

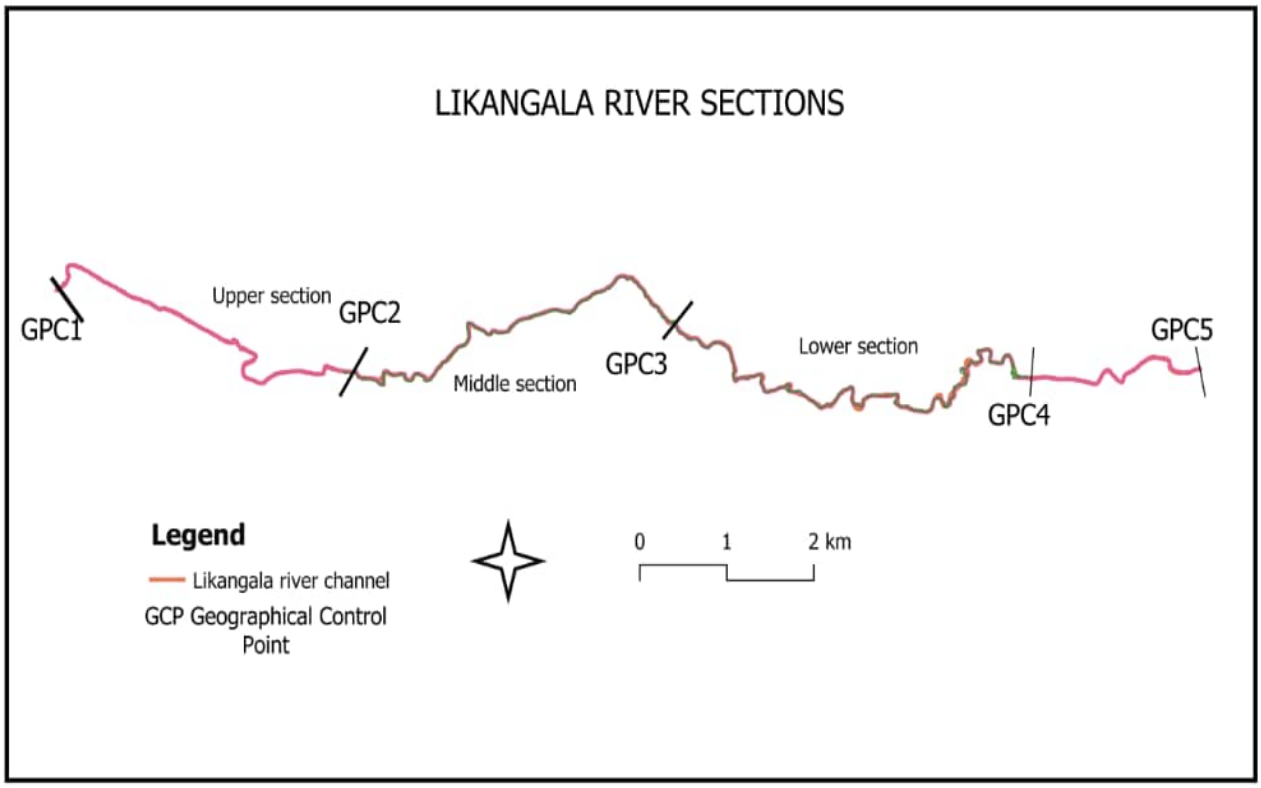
Where, Lcmax is the length of the midline of the channel (in single-channel rivers), or the widest channel (Multiple channel rivers). And LP is the overall length of the reach.

For calculation of river sinuosity Index, river was divided into three segments as upper, middle and lower (Fig. 3). Polygons were converted into the polylines and the field geometry was calculated to know the river length while the Measure Tool was used to measure the shortest length (XY) and Field Calculator was used to calculate the sinuosity index in ArcGIS environment. Some GCP (Ground Control Point) was selected on the left bank of 2007 river course and based on the measured direction distance between GCP and river course was measured during study and it was been estimated how much river in which direction shifted during study duration.

Table 3: GPS coordinates for selected sites

Section of study area	Distance (km)	Site number	Coordinate at NAD83/WGS84
Upper	3.95	1	36L E 744703.6 N 8296330.2
		2	36L E 747519.4 N 8295493.4
Middle	3.87	3	36L E 749701.7 N 8295896.5
		4	36L E 749373.9 N 8295758.3
Down	7.00	5	36L E 751166.3 N 8296461.5
		6	36L E 752258.9 N 8295437.9

Figure 5: Geographical control points on Likangala River



4. RESULTS AND DISSCUSSIONS

This section presents and discusses results of LULC and hydro-meteorological characteristics of the Likangala watershed. The section also discusses the relationship that exists between the LULC, hydro-meteorological characteristics and morphological characteristics of Likangala river.

4.1. Changes in land use and land cover (LULC) in the Likangala river basin from 1993 to 2022.

4.1.1. Ground truth accuracy assessment

The classified land use land cover maps obtained after pre-processing and supervised classification images are displayed in **Figure 5**. The ground truth data obtained from Google Earth Pro was used to verify the classification accuracy. Cited in Kapatamoyo, et al., (2023), Batar, Watannabe & Kumar, (2017), states that accuracy assessment is a substantial step in the LULC classification process. It aims at quantitatively evaluating how effectively pixels are grouped into the correct feature classes in the study area. For this study, the reference datasets are presented in table 4. A set of 117, 99, 75 and 65 reference points were generated using stratified random sampling in SCP, based on the sizes of the LULC classes for 1993, 2002, 2013, and 2022 classified maps respectively. The total number of samples (reference points) per each classified image was calculated using the equation by (Olofsson et al., 2014). This equation was also used by Kapatamoyo, et al., (2023) during his study on Lilongwe city. The total number of reference points were then multiplied by the proportion of each LULC class.

Table 4: shows details of reference points for each LULC class.

LULC Class	Reference points			
	1993	2002	2013	2022
Vegetation	35	25	15	15
Water	0	5	6	5
Built up area	20	15	10	10
Bare land	41	24	24	20
Barren land	21	30	20	15
Total	**117**	**99**	**75**	**65**

Equation 13: Number of reference points per classified image

$$N = \sum i = 1[\frac{(WiS * 0Si)}{So}]2$$

Where:

Wi = mapped area proportion of class i

Si = standard deviation of stratum i

So = expected standard deviation of overall accuracy

C = total number of classes.

Table 5: 1993-2022 accuracy % table

LULC	Accuracy (%)
1993	87.3
2002	90.5
2013	91.7
2022	95.1

4.1.2. LULC Change detection technique

According to (Manyungwa, 2023), Urban landscapes are a complex blend of different features such as buildings, roads, vegetation, and water. The complexity of urban environments leads to mixed pixels in coarse and medium spatial resolution remotely sensed satellite images (Zhang, Chen, & Lu, 2015) , such as the 30m spatial resolution Landsat imagery used in this study. Cited in Manyungwa, (2023), (Lu, Moran, & Hetrick, 2011), found that mixed pixels have been identified as a barrier to efficiently using remotely sensed data in land use land cover classification and change detection. When using pixel-based classification methods, such as the RF method used in this study, the presence of mixed pixels leads to the overestimation and underestimation of the land area of land cover classes depending on the 28 dominant LULC type in the subsection of the study area. This confusion was not unique to undeveloped and developed land but extended to other class types. The sources of misclassification in LULC change detection studies make it difficult to accurately measure the exact changes in area coverage of the different LULC types. Nonetheless, the post-classification change results reveal general land use land cover patterns and historical trends in a study area. Analyzing the historical trends can provide significant information to understand the dynamics of the changing urban landscape and

support future planning activities. The assessment also serves as a basis for forecasting and addressing any future challenges associated with LULC.

4.1.3. Calculation of annual rate of change

To calculate the annual rate at which land use change is taking place, the study adopted a method by malik & Bhat, (2014). According to Kapatamoyo, et al., (2023) the equation gives a standard for comparing Land use changes that are not susceptible to different periods between study periods. A negative value signifies the decrease of a particular LULC class in a given period while a positive value indicates an increase of a specific class at a particular annual rate of a given period. On the other hand, a 0 denotes that the annual rate of change for a particular LULC class remained constant.

Equation 14: Calculating annual rate of change

$$r = [\frac{(Lb - La)}{La} * \left(\frac{1}{T}\right) * 100$$

Where;

r = The annual rate of change

La = Amount of the LULC category in the year a.

Lb = Amount of the LULC category in the year b.

T = Length of time between year a and b.

4.1.4. Urban expansion

The increased built-up area coverage of the developed LULC is immediately apparent through the visual interpretation of the LULC thematic maps in figures 5 (1993, 2002, 2013 and 2022) below.

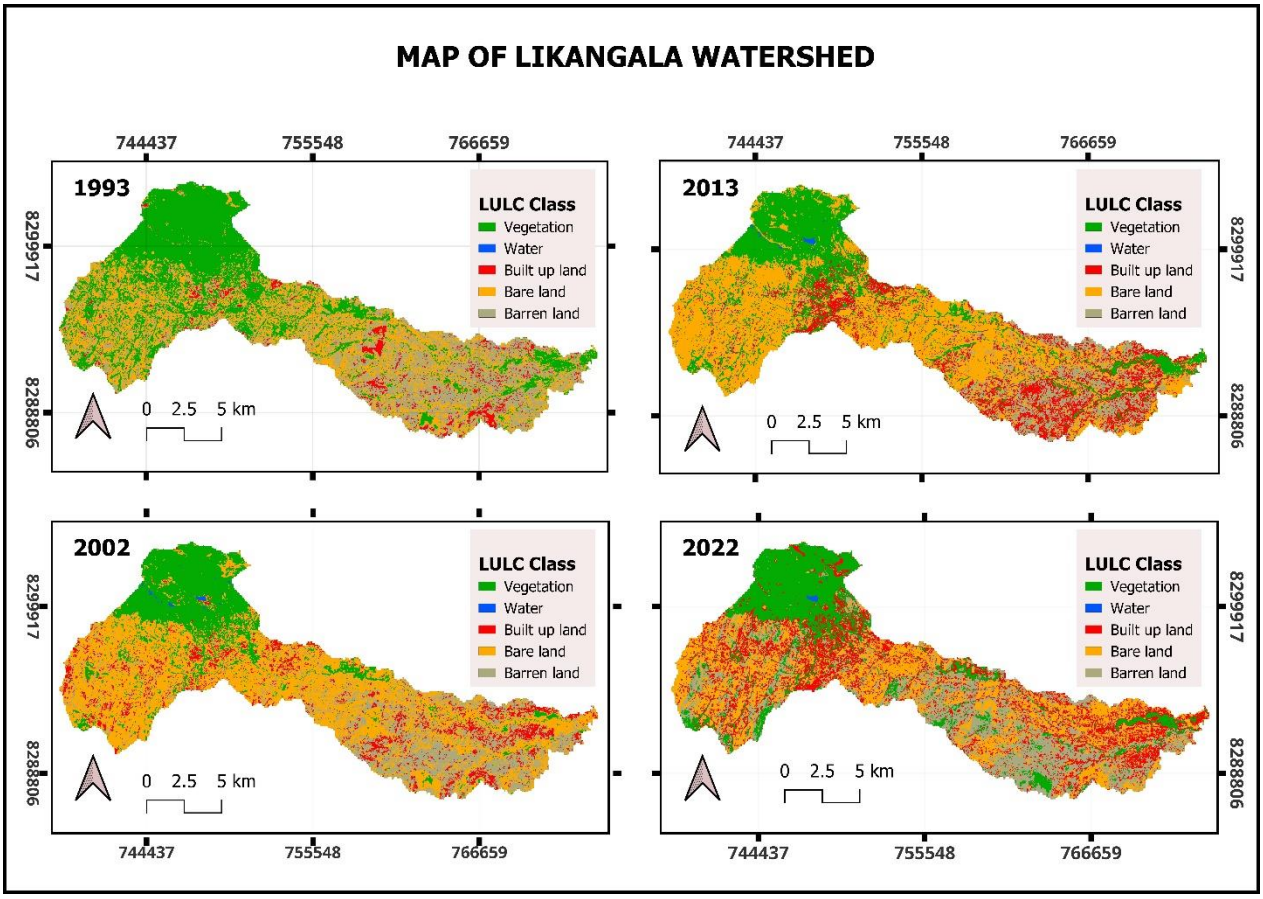


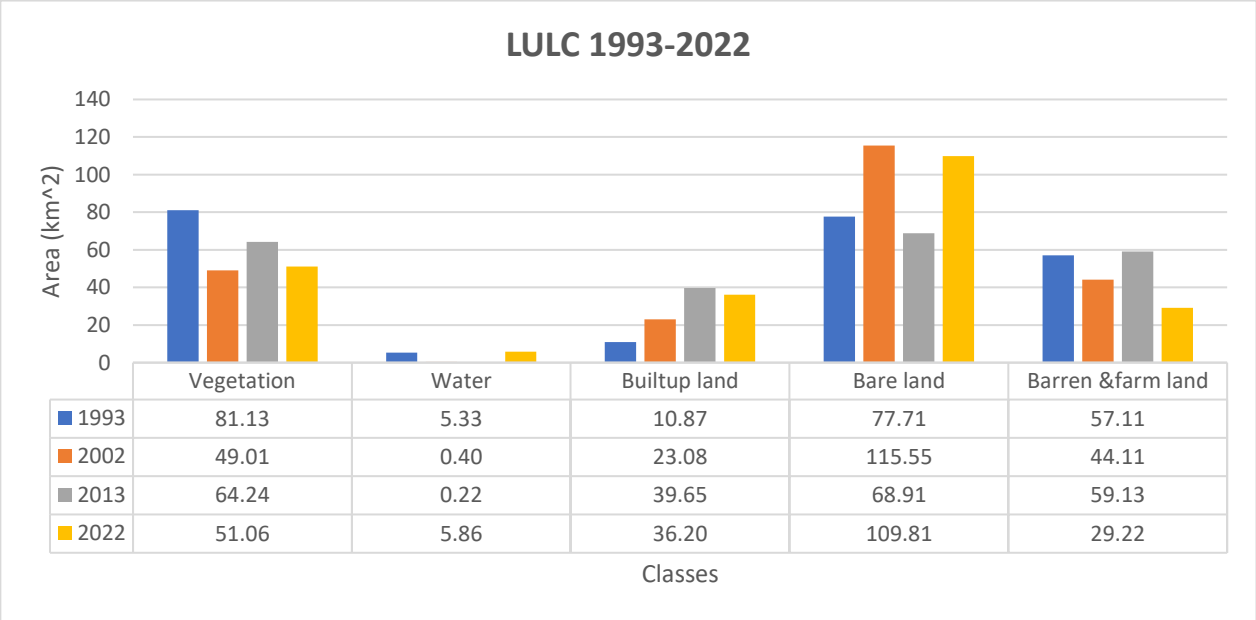
Figure 6: Map of the study area

Image statistics indicate that the area and percent coverage of developed LULC kept on increasing from 10.87km^2, 23.08km^2, 39.65km^2, and 36.02km^2 in 1993, 2002, 2013 and 2022 respectively. This indicates that urban growth has occurred throughout the specified period, from 5%, 10%, 17% to 16% of the total surface area of watershed in these three decades respectively. LULC statistics indicates a decrease in built-up land from 2013 to 2022. This may be due to loss of buildings to cyclones and floods that occurred in 2014 and 2019 (Malawi Government, 2019). The development or extension of pre-existing built-up clusters and the bare land which comprise of farmed area east of the city are two major features of the urban expansion. This shows how unoccupied land parcels inside and outside of established urban clusters are occupied. While built up area expansion is evident across the watershed, the northeast, southeast, south and southwest regions all had rather large increase. The rapid urbanization and lack of proper land use planning has led to an increase in the informal settlements and unsafe housing development in the city (UN-HABITAT, 2011). This is complemented by Ngalande and Odera (2023) who found that the concentration of urban growth in the periphery of the cities in Malawi with reference to

Lilongwe city is due to the increase in rural-urban migration, which leads to high demand for residential housing. The inconsistent supply of plots in designated residential areas and the higher development cost in Traditional Housing Areas lead to migrants being drawn to the informal settlements in the city's edges (Ngalande & Odera, 2023).

The map also shows that urban growth was less concentrated in the northwest part of the city. This is because this part of the city consists of Zomba mountain which is characterized by strict enforcement of urban development regulations and dispersed development. On the other hand, the eastern, southern part of the city is currently occupied by buildings because people have built their houses in the then bare lands and areas that were being used for cultivation.

Figure 7: Post-classification LULC change detection



	Vegetation	Water	Builtup land	Bare land	Barren &farm land
1993	81.13	5.33	10.87	77.71	57.11
2002	49.01	0.40	23.08	115.55	44.11
2013	64.24	0.22	39.65	68.91	59.13
2022	51.06	5.86	36.20	109.81	29.22

Figure 8: Temporal variations in LULC of Zomba city_1993-2022

Table 5 presents the LULC change summary of the conversion from a particular land use land cover to another category. The results indicate that 49.52% of the watershed's landscape remained unchanged between 1993 and 2022. The most significant change in LULC was transforming 40.99% of the landscape from undeveloped land to bare and developed. This indicates increased human activities and the occupation of vacant land. Increased human activity has attributed to 6.59% population growth rate of Zomba city annually, which led to the population growing from 65,915 to 116,797 between 1998 and 2023 alone (National Statistical Office, 2023; Strachan et al., 2021, (UNIMA, 2024). Population growth leads to LULC changes, particularly the growth of the built-up

environment, as humans alter the environment to cater to the growing population's needs. This is evident in Zomba, as evidenced by visual and statistical interpretation of the results.

Table 5: Land use/land cover changes result depicting area change and annual rate of change for the study periods (1993–2022).

LULC	Cover change Rate change gain(+) rate change loss (-)/year				
	2002-1993	**2013-1993**	**2022-1993**	**2013-2002**	**2022-2013**
Vegetation	-32.12	-16.89	**-30.07**	15.23	-13.18
Water	-4.93	-5.11	**0.53**	-0.18	5.64
Built up land	12.21	28.78	**25.33**	16.57	-3.45
Bare land	37.84	-8.80	**32.10**	-46.64	40.90
Barren land	-13.00	2.02	**-27.89**	15.02	-29.92

Table 6: 1993-2022 Land Cover Change matrix (km2)

	New Classes (2022)					
Reference Class (1993)	Vegetation	Water	Built up	Bare land	Barren/ cultivated	Total
Vegetation	**47.07**	0.41	64.90	31.05	14.45	86.46
Built up	0.24	0	**25.06**	4.54	3.59	10.87
Bare land	72.80	0.001	14.01	**48.81**	75.97	77.71
Barren/cultivated	1.45	0	13.20	25.88	**16.58**	57.11
Total	56.03	0.42	36.21	110.27	29.22	**618.32**

The results also indicate that the developed LULC changed to different categories, with 1.1367 km^2 representing 2.71% change of the watershed landscape from developed to undeveloped land followed by a change of 3.31% to vegetation, being the most significant.

4.2. Hydro-metrological trends of the Likangala watershed from 1993 to 2022

4.2.1. Rainfall

Precipitation trends in the study region are gleaned from a preliminary quantitative analysis of rainfall data from 1993 to 2022. Likangala received 1160.913mm of annual rainfall on average throughout this time, with a 19.07% coefficient of variation. This suggests that the yearly amounts of rainfall vary quite a little. In addition, there are two separate seasons: the rainy season has an average rainfall of 1122.23 mm, while the dry season has an average

of 38.68 mm. It's important to remember that terrain greatly influences rainfall patterns; this is especially true in places like Malawi (Chauluka, Singh, & Kumar, 2020).

Table 7: Summary of Mann-Kendall test results of monthly and seasonal Rainfall data from 1993-2022

Month	Kendall's tau	S	P-value	Trend
January	-0.092	-40.0	0.487	Decreasing
February	-0.529	-23.0	0.695	Decreasing
March	-0.002	-10.0	0.100	Decreasing
April	-0.161	-70.0	0.218	Decreasing
May	-0.472*	-196.0	0.0004	Decreasing
June	-0.430*	-166.0	0.0018	Decreasing
July	-0.470*	-188.0	0.0005	Decreasing
August	-0.375*	-127.0	0.009	Decreasing
September	-0.378*	-123.0	0.009	Decreasing
October	-0.100	-43.0	0.453	Decreasing
November	-0.067	-29.0	0.617	Decreasing
December	-0.140	-61.0	0.284	Decreasing
Annual	-0.255*	-111.0	0.050	Decreasing
Wet-season	-0.228	-99.0	0.080	Decreasing
Dry-season	-0.421*	-183.0	0.001	Decreasing
NOTE: The * show significance at 5%				

Table 8: Sen's Slope test results for monthly, annual and seasonal rainfall from 1993-2022

Month	Sen's slope
January	-1.426
February	-1.181
March	-0.124
April	-0.957
May	-0.225
June	-0.125
July	-0.133
August	0.0
September	0.0
October	-0.208
November	-0.375
December	-2.689
Annual	-0.164
Wet-season	-6.000
Dry-season	-1.685

Table 9: Summary of Mean, Std. deviation and Coefficient Variation % for Rainfall data from 1993-2022

Variable	Mean	Std. deviation	Coefficient Variation (%)	Interpretation
Jan	319.22	104.13	32.62	Moderate
Feb	253.71	107.38	42.33	High
Mar	180.42	97.47	54.03	High
Apr	50.22	38.11	75.89	High
May	6.27	11.49	183.31	Extremely high
Jun	3.22	4.49	139.51	Extremely high
Jul	4.93	10.01	203.14	Extremely high
Aug	1.76	3.40	192.77	Extremely high
Sep	2.10	5.29	251.75	Extremely high
Oct	20.40	22.77	111.59	Extremely high
Nov	82.15	53.00	64.52	High
Dec	236.51	98.87	41.80	High
Annual	96.74	18.44	19.07	Low
Dry Season	6.45	5.59	86.77	High
Wet Season	187.04	35.41	18.93	Low
NOTE CV %: 0-20 means low, 21-40 means moderate, 41-60 means high and 60 above means extremely high				

4.2.1.1. Annual, seasonal and monthly rainfall trend

The annual rainfall from 1993 to 2022, expressed in millimeters, is depicted in the following graph. Significant variations in rainfall levels throughout this time period are shown by each blue open dot, which represents the reported rainfall for a particular year. There were years with high rainfall, such 1995 and 2007, and years with much less rainfall, like 1994 and 2018. There has been a little decrease in yearly rainfall throughout the years, as seen by the black line on the graph, which is a linear trend line fitted to the data points. The general trend indicates that, from 1993 to 2022, the annual rainfall has been progressively decreasing, notwithstanding the annual changes.

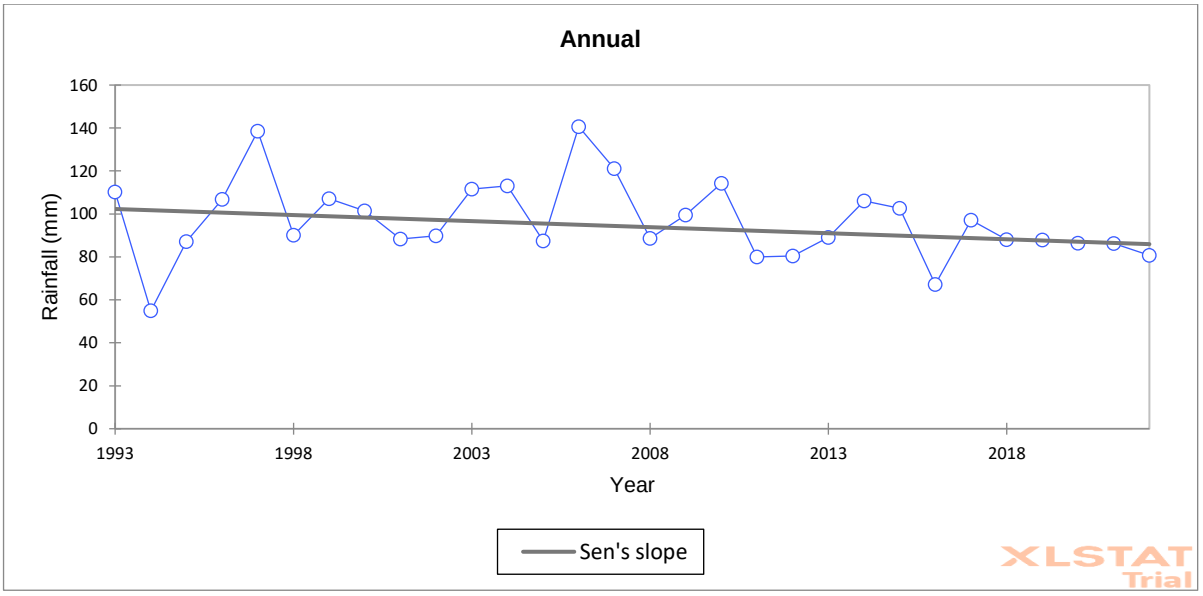


Figure 9: The annual rainfall trend from 1993 to 2022

The annual rainfall during the dry season, expressed in millimeters, is shown on the Dry Season graph from 1993 to 2022. Each black open dot on the graph represents the rainfall for a particular year. There have been considerable variations, with negligible rainfall in years like 1994, 2012, and 2016 and notable maxima around 1997 and 2002. Despite annual differences, the black trend line shows an overall drop in rainfall over time, indicating that the dry season has been progressively drier from 1993 to 2022.

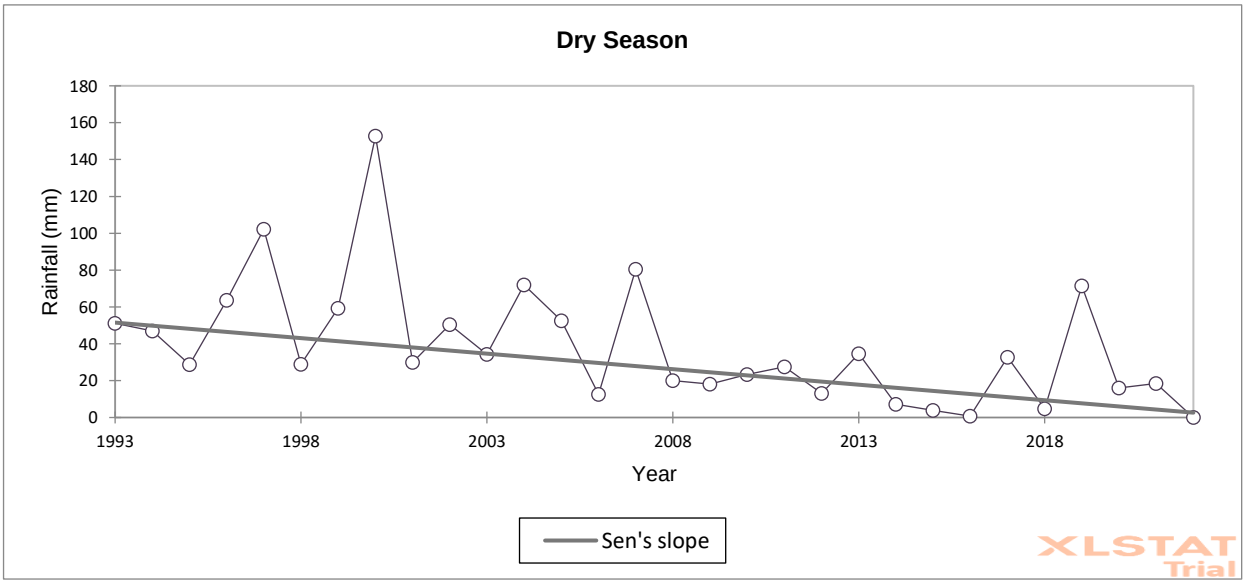


Figure 10: Rainfall trend for dry season from1993 to 2022

The wet season graph shows the annual rainfall in millimeters during the rainy season from 1993 to 2022. Each red dot on the graph represents the rainfall for a particular year. There are noticeable variations, with lesser rainfall in years like 1994 and 2016 and prominent peaks around 1997, 2006, and 2010. Despite annual variances, the brown trend line shows an overall drop in wet season rainfall over time, indicating that the wet season has steadily becoming drier from 1993 to 2022.

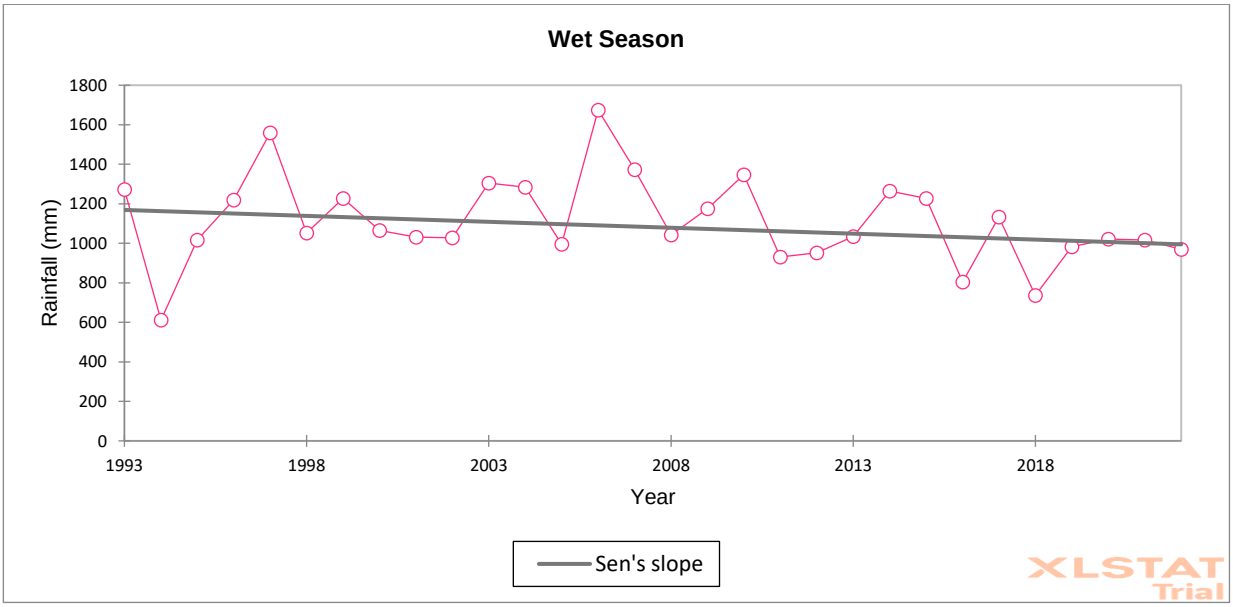


Figure 11: Rainfall trend for dry season from 1993 to 2022

4.2.1.2.Change detection for the annual, seasonal and monthly rainfall

Considerable variations in annually and seasonal precipitation are shown by analyzing rainfall patterns from 1993 to 2022. The pattern throughout time indicates a constant decrease in rainfall, even with year-to-year variability. Like the rainy season, the dry season has general decreasing direction with periodic rises. There may be an influence on the local ecosystems and water resources as a result of this change towards drier circumstances.

4.2.1.3. Change point detection for the monthly rainfall

The Pettit test for monthly rainfall exhibits no change in January, February, March, April, November and December. There was a prevalent significant downward change from May to September with change points in 2013, 2014, 2011, 2005, and 2007. As seen clearly, these changes occurred between 2005 and 2014. During this period the country experienced weather fluctuations. The country was struck by drought in 2005, as evidenced

by the majority of change points between 2005 and 2014. Many parts of the country, including Zomba district, were affected, leading to a famine of 4.7 million people (Chauluka, Singh, & Kumar, 2020). There were no change points in January, February, April, November, and December. The results reveal that the amount of rainfall received during these months of the wet season has relatively remained the same over the 30 years. At the same time, there is minimal inter-annual monthly variability of the rainfall in the catchment.

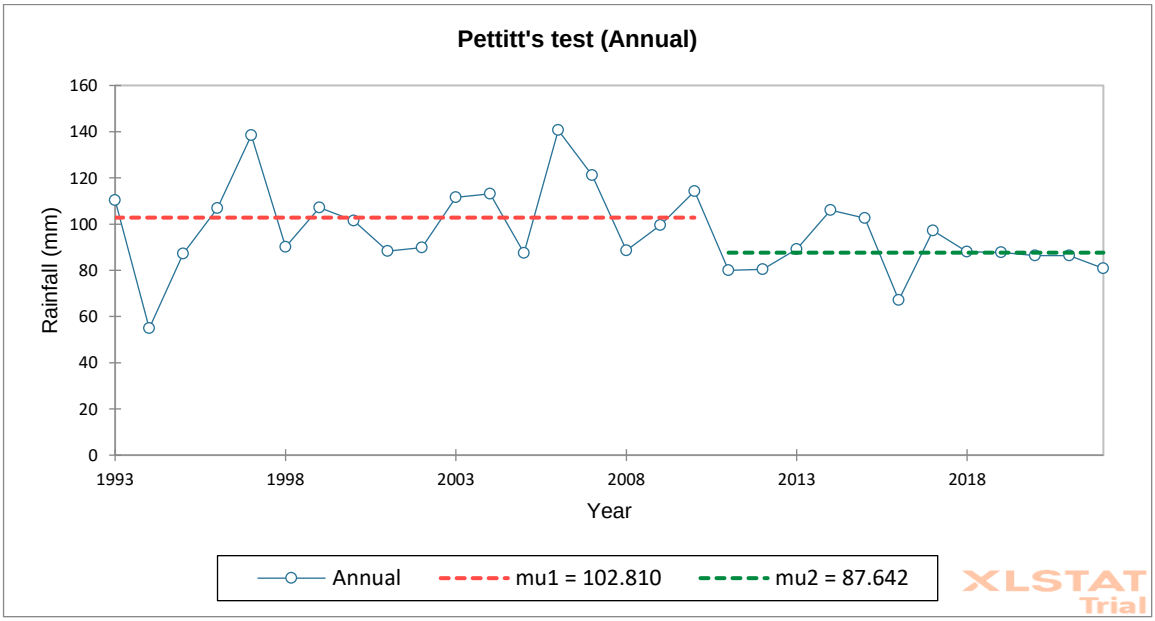


Figure 12: The Pettit homogeneity test of the annual rainfall.

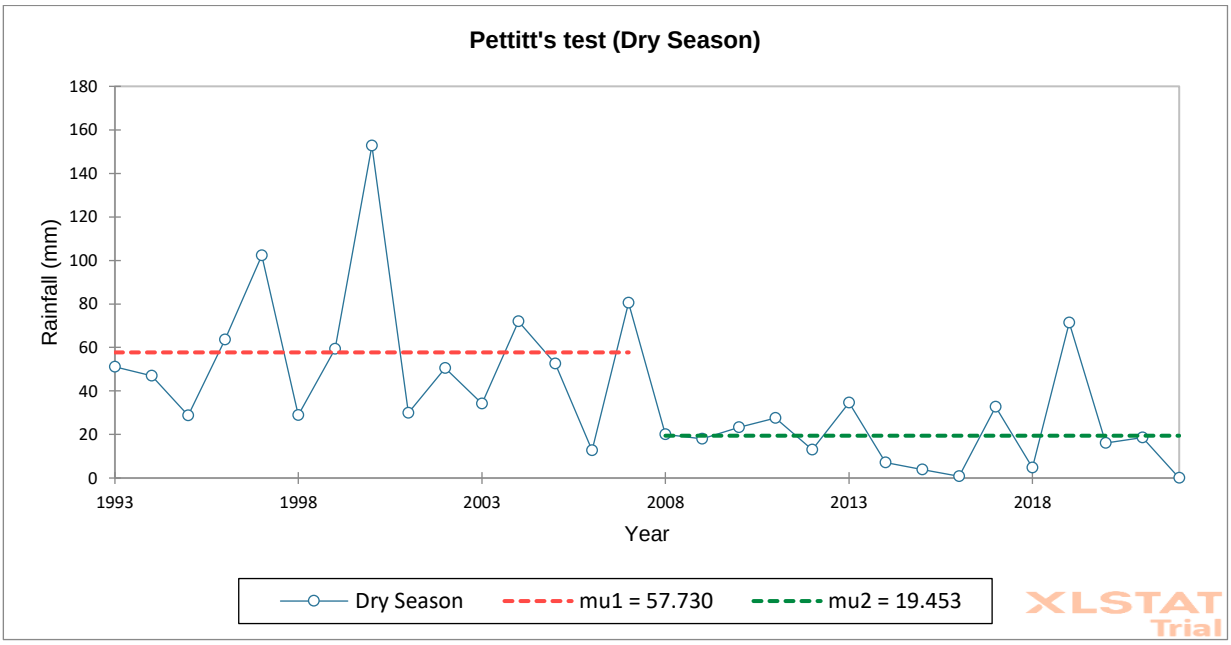


Figure 13: The Pettit homogeneity test of the dry season.

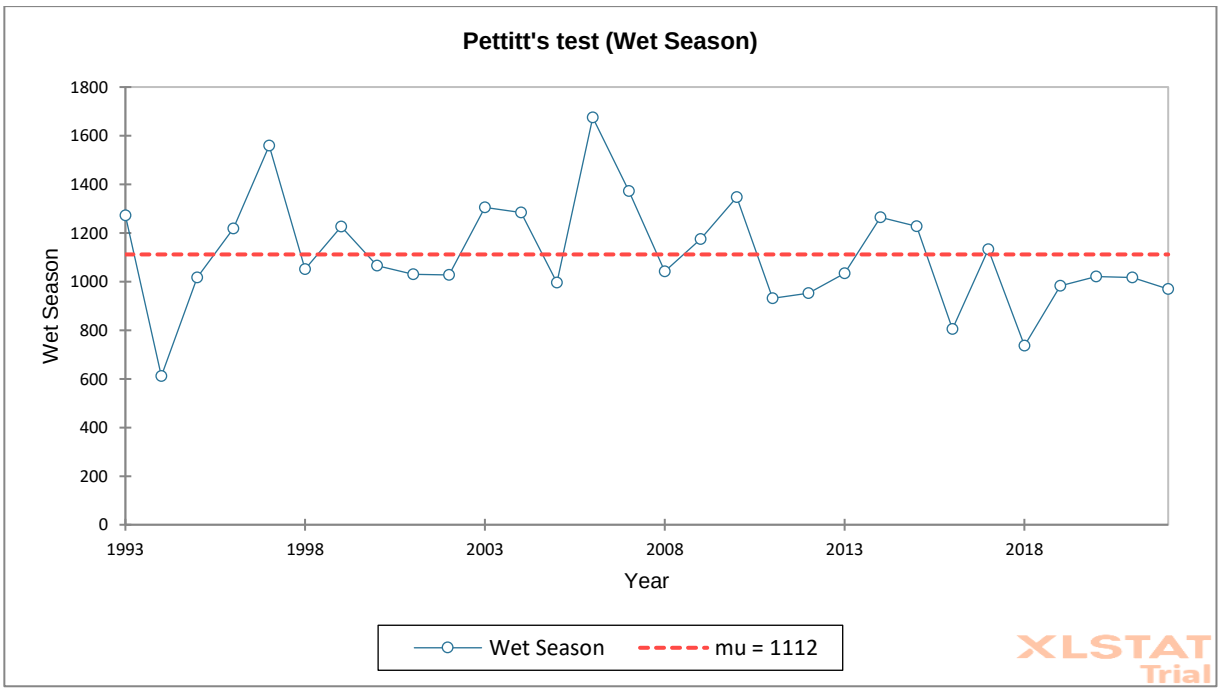


Figure 14: The Pettit homogeneity test of the wet season.

4.2.2. Streamflow

The mean annual streamflow for the Likangala River at Mkokangowo gauging station ranged from 26.26 m3/s to 131.27 m3/s at its peak and lowest points between 1997 and 2022. A coefficient of variation of 60.42% is associated with the river's typical annual streamflow of 125.4 m3/s. A mean streamflow of 3.35 was observed during the dry season and 82.08 during the rainy season.

Table 10: Summary of Mann-Kendall test results of monthly and seasonal streamflow data from 1993-2022

Month	Kendall's tau	S	P-value	Trend
January	-0.269*	-117.00	0.038	Decreasing
February	-0.080	-35.00	0.544	Decreasing
March	0.338*	147.00	0.009	Increasing
April	0.559*	243.00	0.0002	Increasing
May	0.237	103.00	0.069	Increasing
June	0.398*	173.00	0.002	Increasing
July	0.729*	317.00	0.000	Increasing
August	0.090	39.00	0.500	Increasing
September	0.037	16.00	0.788	Increasing
October	0.195	85.00	0.134	Increasing
November	0.099	43.00	0.454	Increasing
December	-0.039	-17.00	0.775	Decreasing
Annual	-0.002	-1.00	1	Decreasing
Wet-season	-0.016	-7.00	0.915	Decreasing
Dry-season	0.476*	-207.00	0.0002	Increasing
NOTE: The * show significance at 5%				

Table 11: Sen's Slope test results for monthly, annual and seasonal streamflow from 1993-2022

Month	Sen's slope
January	-3.104
February	-0.671
March	1.881
April	1.030
May	0.109
June	0.070
July	0.164
August	0.008
September	0.0004
October	0.139
November	0.196
December	-0.083
Annual	-0.005
Wet-season	-0.037
Dry-season	0.094

Variable	Mean	Std. deviation	Coefficient Variance %	Interpretation
Jan	118.00	131.65	111.57	Extremely high
Feb	86.37	67.96	78.69	Extremely high
March	54.95	34.60	62.96	Extremely high
April	18.12	11.75	64.83	Extremely high
May	3.88	4.41	113.58	Extremely high
June	1.88	2.49	132.33	Extremely high
July	1.84	1.65	89.32	Extremely high
August	1.11	0.66	59.12	High
Sep	0.74	0.79	106.77	Extremely high
Oct	10.66	6.85	64.23	Extremely high
Nov	53.40	19.46	36.43	Moderate
Dec	161.65	35.35	21.87	Moderate
Annual	42.72	19.03	44.55	High
Wet season	82.08	36.82	44.86	High
Dry season	3.352	2.03	60.42	Extremely high
NOTE CV %: 0-20 means low, 21-40 means moderate, 41-60 means high and 60 above means extremely high				

Table 12: Summary of Mean, Std. Deviation, coefficient Variance %

4.2.2.1. Annual, seasonal and monthly streamflow trend

The graph illustrates the notable variations in discharge rates over time by showing the yearly discharge from 1993 to 2022. A noteworthy high is observed around 1998, when the discharge reaches around 135 units, and another noteworthy peak is observed around 1995, when the discharge reaches about 80 units. The trend line shows a modest declining tendency in discharge across the whole time, notwithstanding these variations. After around 2010, the discharge rates seem to have stabilized, often ranging from 30 to 50 units, with less notable peaks. The yearly discharge appears to be gradually declining, stabilizing in recent years with less unpredictability, according to this general pattern.

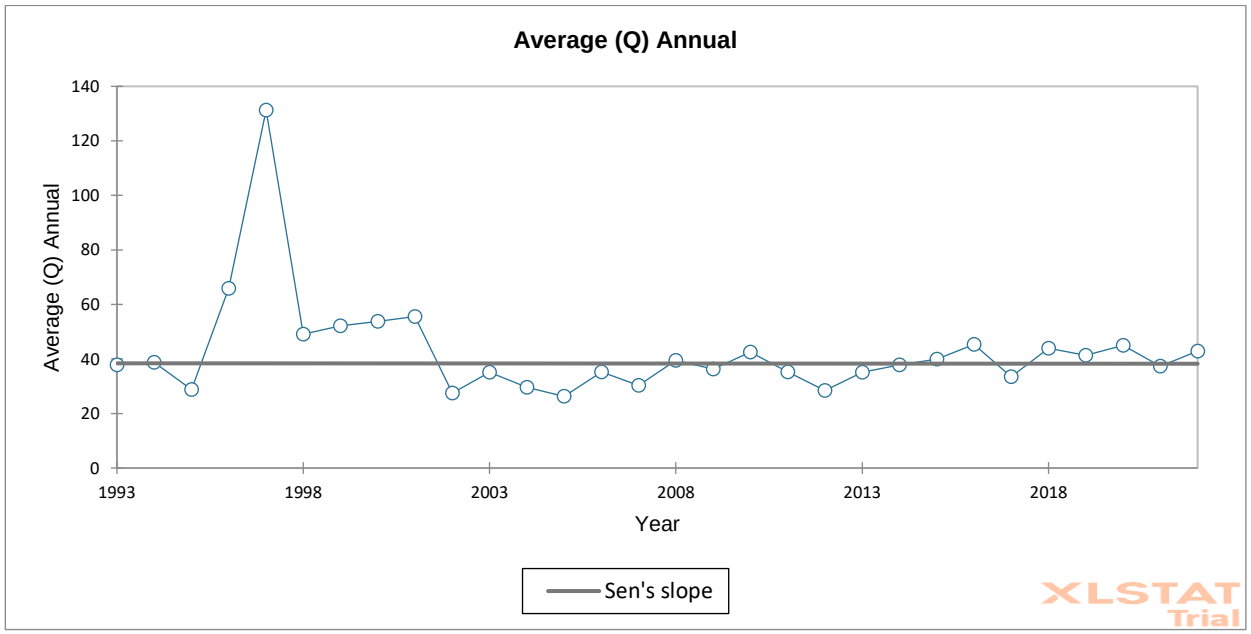


Figure 15: Annual streamflow trend from 1993-2022

The graph shows the major variations in discharge rates during the years from 1990 to 2022 during the rainy season. The discharge peaks at two different times: about 1998, when it is at its greatest point, and around 1995, when it is at its lowest point, about 250 units. The trend line shows a modest declining tendency in discharge across the whole time, notwithstanding these variations. The discharge rates are more constant starting around 2010; they typically fluctuate between 50 and 100 units, with fewer sharp peaks. The general pattern indicates that flow would gradually decline throughout the wet season, stabilizing in recent years with less unpredictability.

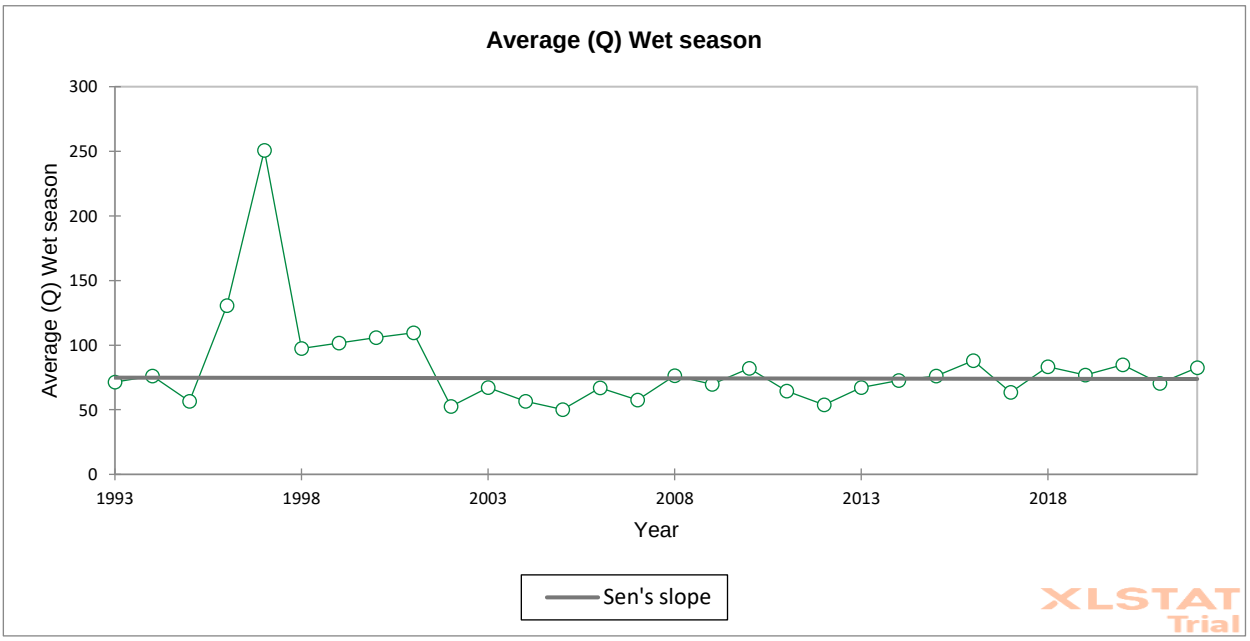


Figure 16: Wet season streamflow trend from 1993-2022

The discharge rates during the dry season from 1990 to 2022 are shown in the graph. The discharge rates vary significantly during this time, with two major peaks that occur around 1998 and 2010 and respectively reaching roughly 13 and 7 units. The trend line indicates a little increase tendency in discharge throughout the years, despite these oscillations. With fewer sharp spikes and a general decline towards 2022, the discharge rates seem to have stabilized in recent years, especially from 2015 onward. This suggests that, notwithstanding a few years with noticeably higher discharge, the general tendency during the dry season is toward a modest rise in discharge during the time period under study.

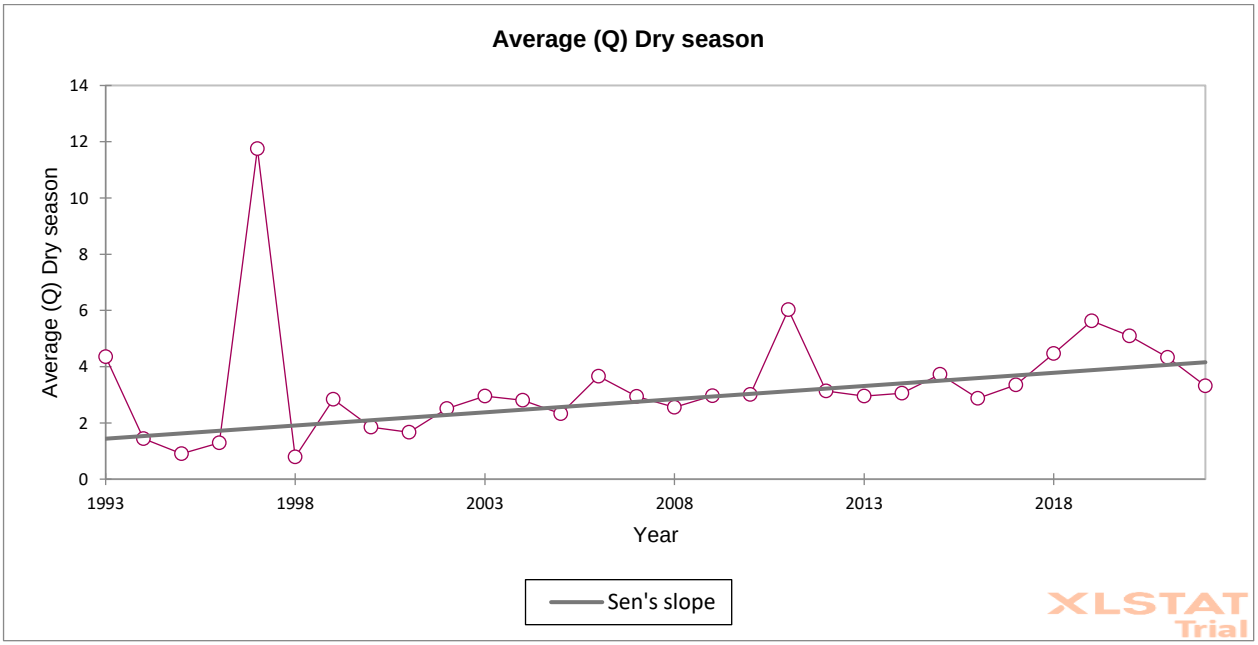


Figure 17: Dry season streamflow trend from 1993-2022

4.2.2.2. Change detection for the annual, seasonal and monthly streamflow

The change detection for streamflow reveals significant trends across annual, seasonal, and potentially monthly data. The annual discharge from 1993 to 2022 shows a slight downward trend with stabilization in recent years, primarily fluctuating between 30 and 50 units. During the dry season, discharge rates display an upward trend with a more stable pattern in recent years, despite notable peaks in 1998 and 2010. Conversely, the wet season shows a slight downward trend with discharge rates stabilizing between 50 and 100 units after 2010, following significant peaks in the late 1990s. Monthly streamflow analysis, although not depicted, would likely reveal trends in seasonal variability and shifts in peak discharge periods, following similar patterns of stabilization and reduced variability in recent years.

4.2.2.3. Change point detection for monthly streamflow

The Pettit test analysis indicates that the majority of the months have no change points for the study period. For instance, February, March, May, June, August, September, October, November, and December have no change points while January, April and July exhibit significant downward change in 2002. This tells us that monthly streamflow has remained constant over the years despite catchment disturbances, such as land cover changes and weather patterns.

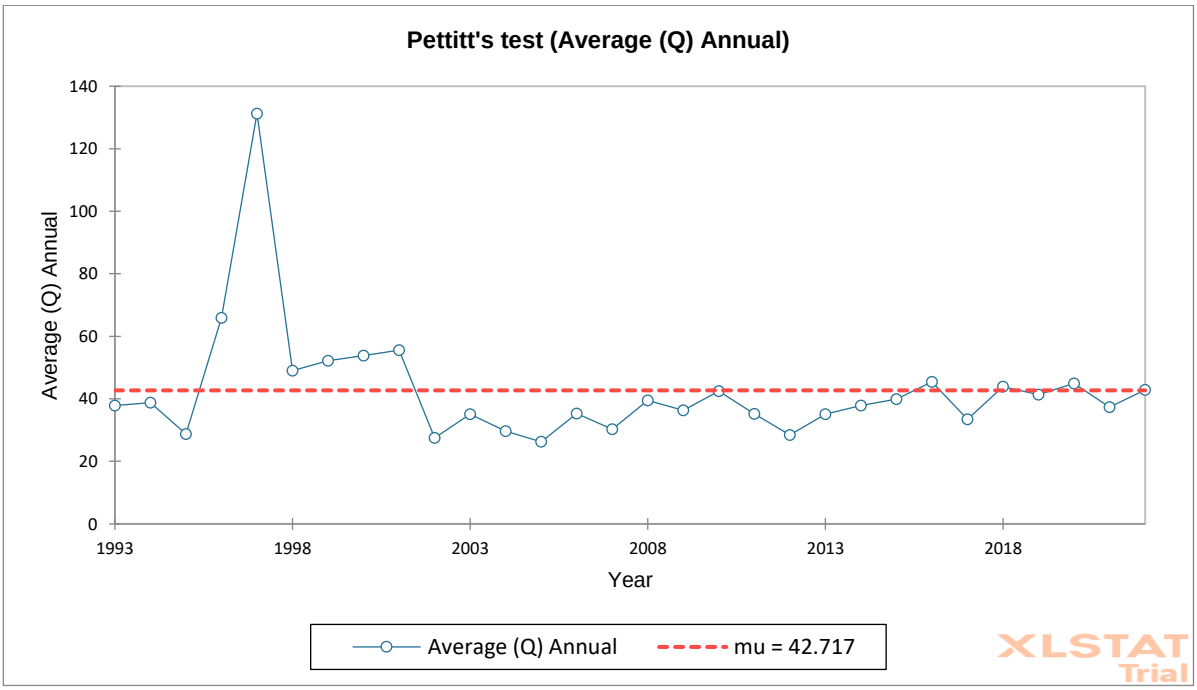


Figure 18: The Pettit homogeneity test of the annual streamflow.

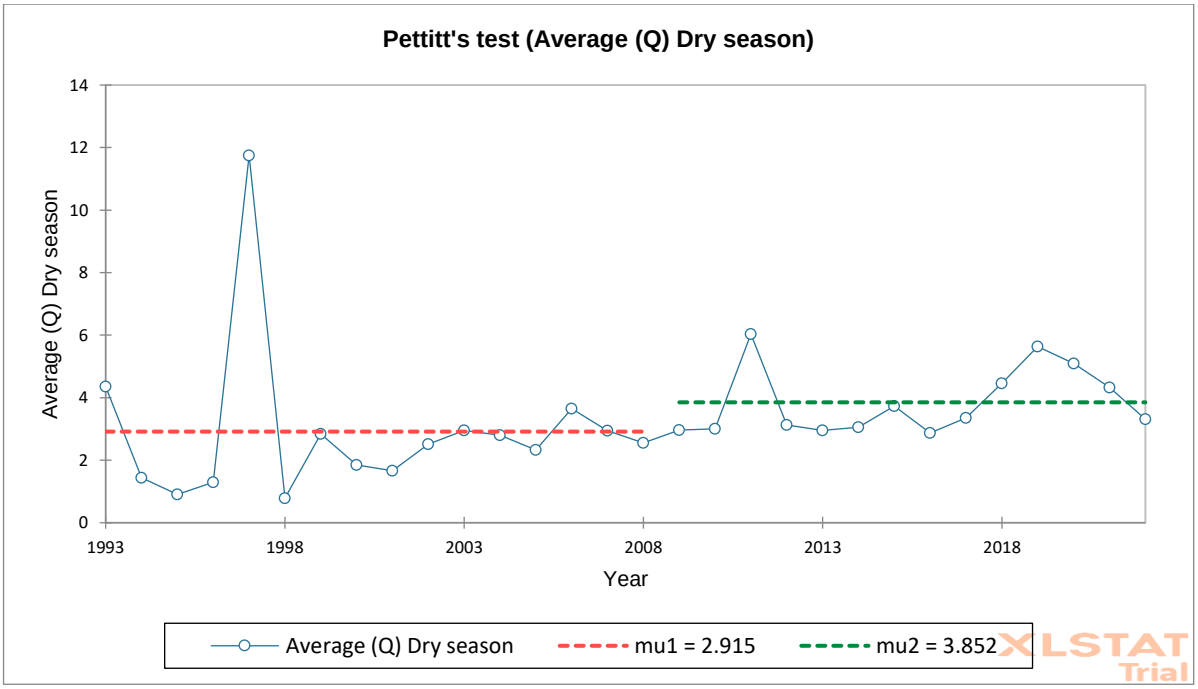


Figure 19: The Pettit homogeneity test of the dry season streamflow.

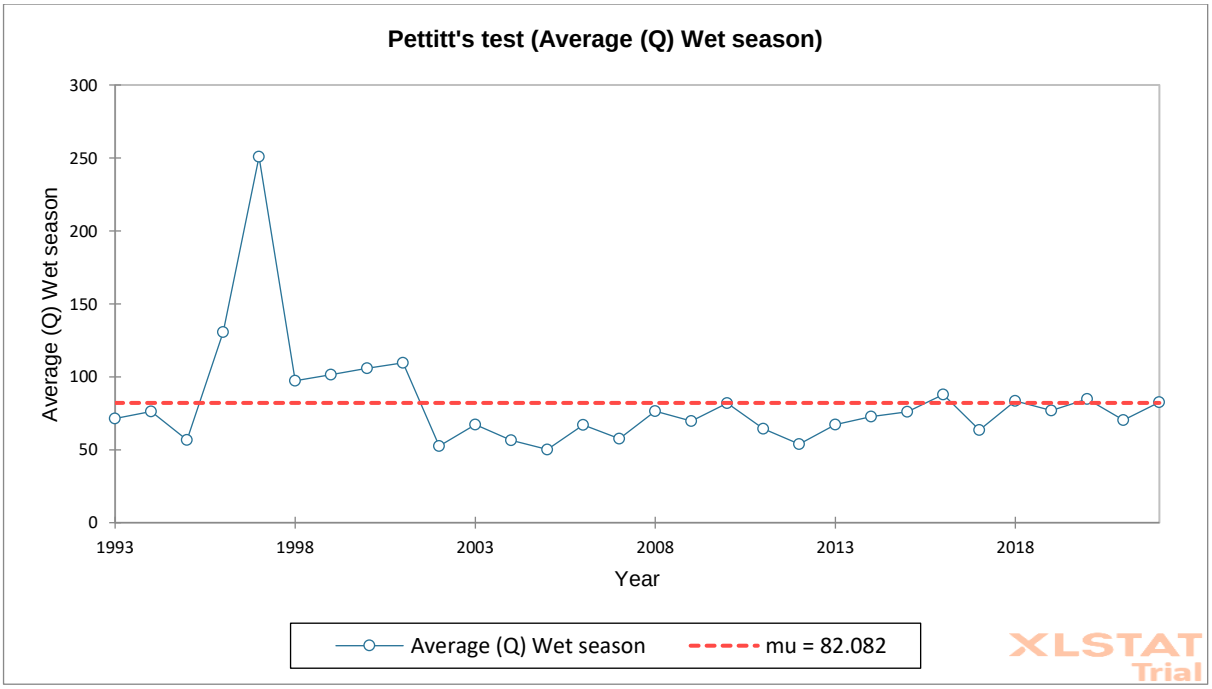


Figure 20: The Pettit homogeneity test of the wet season streamflow.

Relationship between rainfall and streamflow

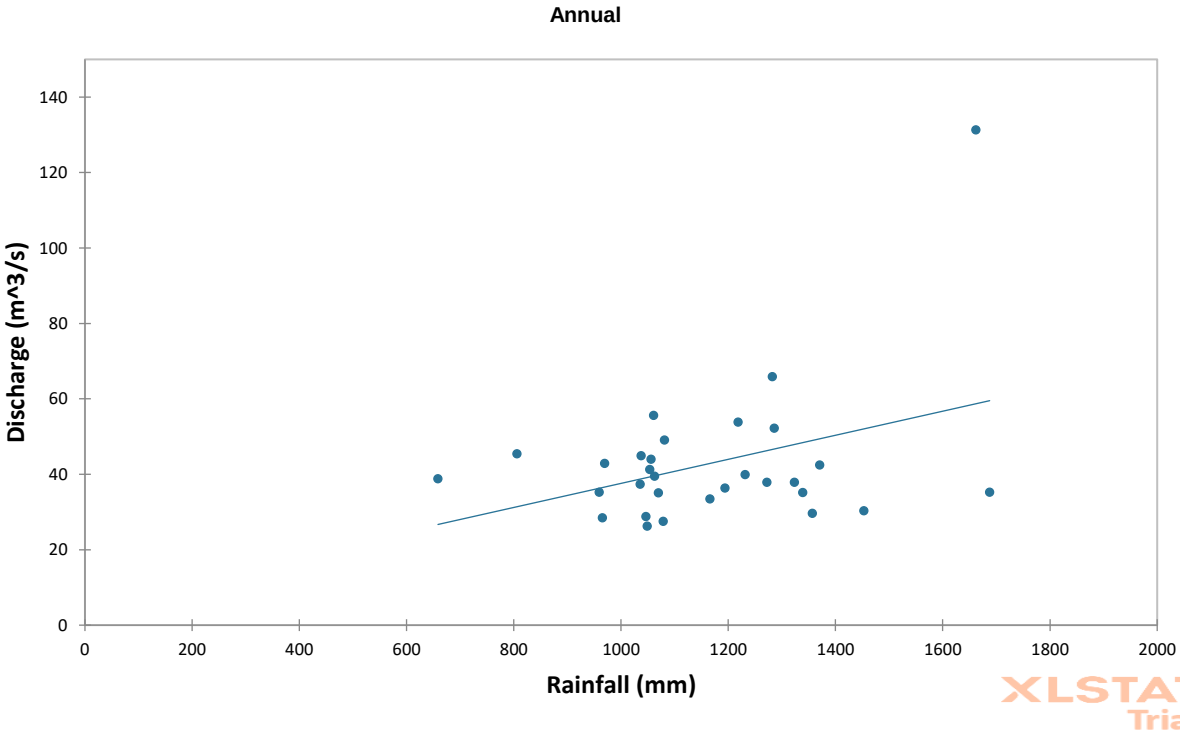


Figure 21: Scatter plots showing the annual relationship between rainfall and streamflow in Likangala River

The graph offers insights into the variability of streamflow with different levels of rainfall by displaying a large number of data points that correspond to certain time periods or locations where both streamflow and rainfall were observed. Since increases in rainfall often result in greater water levels in rivers and streams, the overall trend shows a positive correlation between rainfall and streamflow. A dotted trend line rising from left to right visually depicts this link; nevertheless, it's crucial to remember that correlation does not always indicate causation because streamflow is also influenced by other variables such as soil type, land use, and local terrain. Such graphs are extremely helpful to hydrologists and environmental scientists in their studies of water availability, resource planning, and probable flooding occurrences prediction, all of which improve the efficiency of water systems.

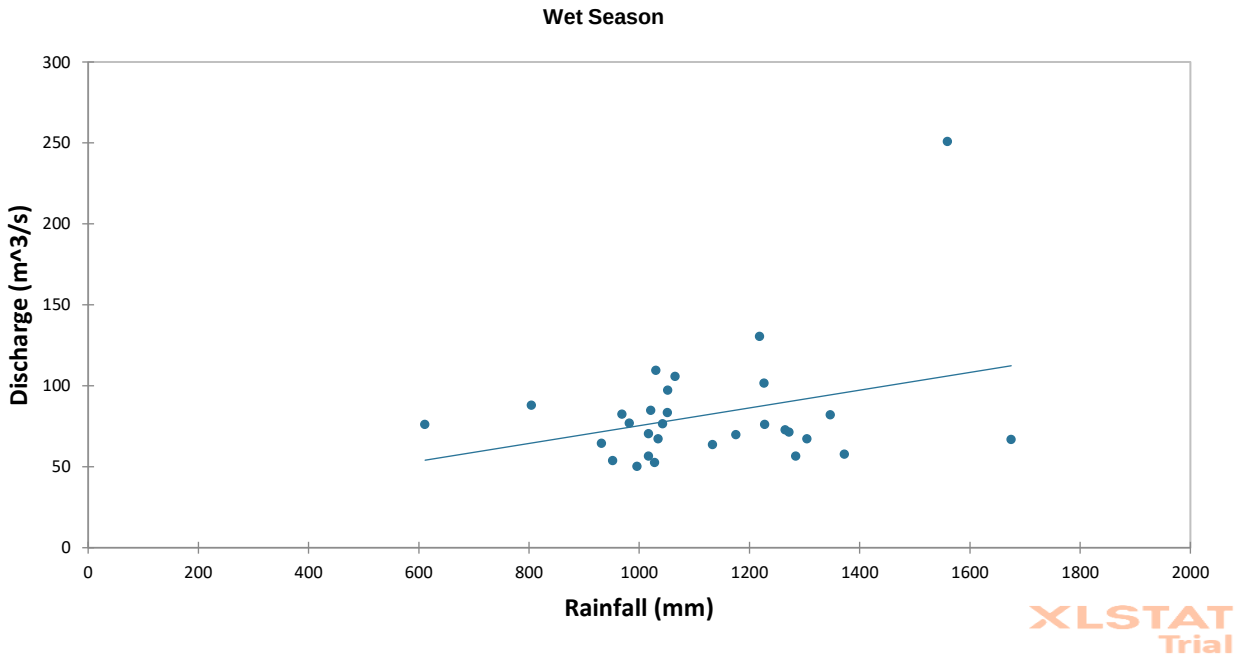


Figure 22: Scatter plots showing the wet season relationship between rainfall and streamflow in Likangala River

Different points of data are represented by a significant number of blue dots dispersed across the graph, each of which connects the streamflow (y-axis) and rainfall (x-axis) in a meaningful way. As a result of heavy rain raising river and stream levels, there is a general pattern of positive association that indicates that more rainfall usually results in increased streamflow. This link is graphically represented by a dotted trend line that ascends from left to right. These kinds of graphs are really helpful to hydrologists and managers of water resources for assessing water availability and forecasting flood hazards based on patterns of precipitation during the rainy season.

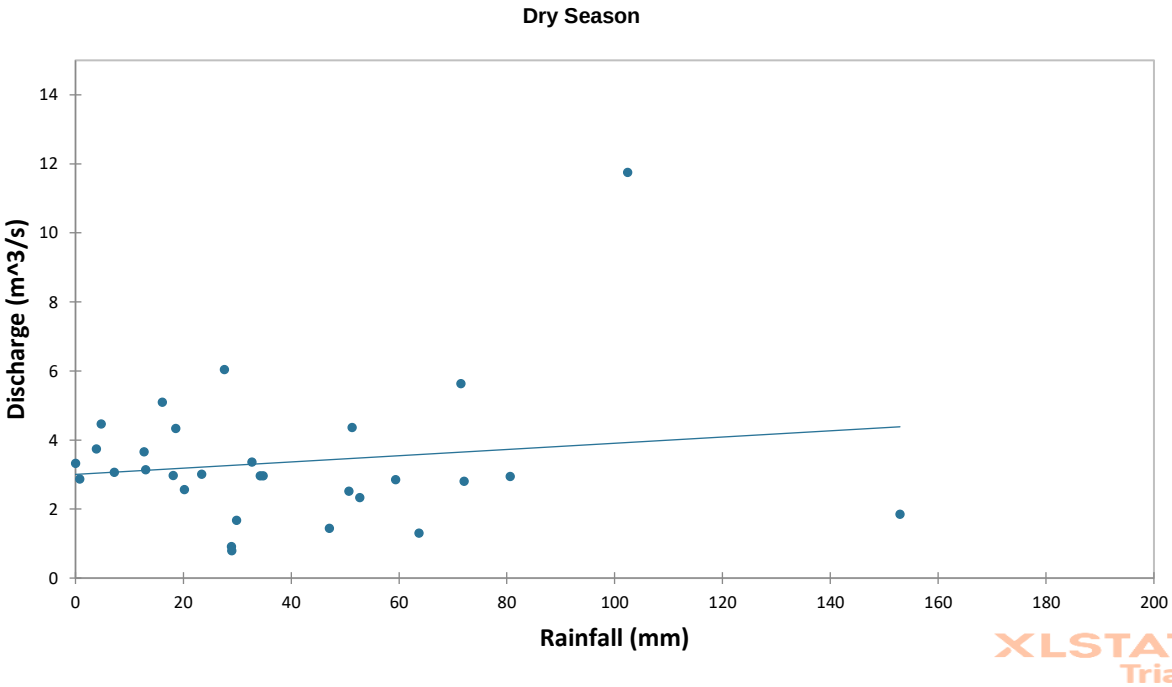


Figure 23: Scatter plots showing the wet season relationship between rainfall and streamflow in Likangala River

The graph's dots show different streamflow readings that match the quantities of rainfall that have been observed. Despite changes in rainfall, the majority of data points cluster in the lower left quadrant, showing generally steady streamflow during the dry season. A dotted line that runs horizontally, slightly slower than 4 m^3/s, indicates a trend line during times of low rainfall. Interestingly, streamflow does not significantly rise as rainfall increases (up to 180 mm), suggesting that rainfall has little effect on streamflow at this particular season or location.

Table: Correlation Rainfall and Streamflow

Month	Correlation Value	P-Value
January	0.1029047	0.5884
February	0.3318529	0.0732
March	0.00064027	0.9973
April	-0.067404	0.7234
May	-0.1410805	0.4571
June	-0.339196	0.0667
July	-0.3611097	0.04993
August	-0.3200518	0.08467
September	0.2702211	0.1487
October	0.4209774	0.02052
November	0.3068725	0.09905
December	0.3450354	0.6185
Annual	0.3709154	0.0436
Wet-season	0.2988741	0.1086
Dry-season	0.1497014	0.4298

4.3. Analysis of correlation between LULC, hydro-meteorological trends, and river morphology variations in the Likangala river

4.3.1. River shifting detection

River course change detection has been done from 2007 to 2022 with consideration of 2007 as base year shown in **Figure 24.** In 2007, the river's upper section measured 8.15 km, while the middle section was 4.26 km and the lower section was 8.55 km. The combined total length of the river for this year was 20.96 km. The sinuosity index, which is a measure of how much the river meanders, was 1.87. This index indicates a relatively meandering river course, suggesting a naturally winding path through the landscape.

By 2013, the lengths of the river sections had changed slightly. The upper section decreased marginally to 8.12 km, the middle section to 4.03 km, and the lower section to 8.15 km. The total river length decreased to 20.30 km. Correspondingly, the sinuosity index decreased to 1.8, indicating a slight reduction in the river's meandering nature. This

reduction in length and sinuosity might be due to a combination of natural processes such as erosion and sediment deposition, or human interventions.

In 2022, the river showed further reductions in length across all sections. The upper section was 8.01 km, the middle section 3.90 km, and the lower section 7.65 km. The total river length had decreased to 19.56 km. Notably, the sinuosity index dropped significantly to 1.5, indicating a considerable straightening of the river course over the years. This marked reduction in sinuosity suggests that the river has become less meandering and more direct in its flow path. Such changes can result from various factors including enhanced sediment transport, increased flow velocity, and possibly deliberate river management strategies aimed at controlling flooding or improving navigation.

It is clear that the maximum river course changed in Lower section at an average of 3512m and the minimum river course changed in the Upper section at an average of 147 m. while the middle section changed at an average of 224m for year 2007 to 2022. It is also observed that many branches have been emerged in the lower section and form the loop, so river course is more curved in this section. Coriolis force caused by the earth's rotation can cause a small imbalance in velocity distribution such that velocity on one bank is higher than on the other (Maurya & Yadav, 2016). This can generate erosion on one bank and deposition of sediment on the opposite bank. The secondary currents cause the flow to proceed in the direction towards eroded portion until redistribution of velocity reverses the process. Stochastic theory ascribes random fluctuations in the flow velocity due to some debris or disturbance to affect velocity distribution across the segments, for the formation of meanders.

Equilibrium theory states that meandering is the process by which a river adjusts its gradient (length along the course divided by the drop in elevation) so that there is an equilibrium between the erodibility of the terrain and the erosive power of the stream (Kundu & Chattopadhyay, 2022).

Geomorphic theory attributes tectonic features acting as obstacles to deflect the stream to cause meanders. It is believed that a necessary condition for the development of meander is erosion of the bed and its subsequent deposition further downstream. This is caused by the secondary currents, generated downstream of a bend, provided of course that the discharge and bed material are favourable for this process.

These observed changes highlight a trend of decreasing river lengths and sinuosity over time. The most pronounced reductions were seen in the lower section of the river, which

may be more susceptible to changes due to its downstream location where sediment accumulation and human activities are often more significant. The overall reduction in sinuosity implies that the river is becoming straighter, which can have significant ecological and hydrological implications, such as altered habitats, changes in sediment transport dynamics, and potential impacts on floodplain connectivity.

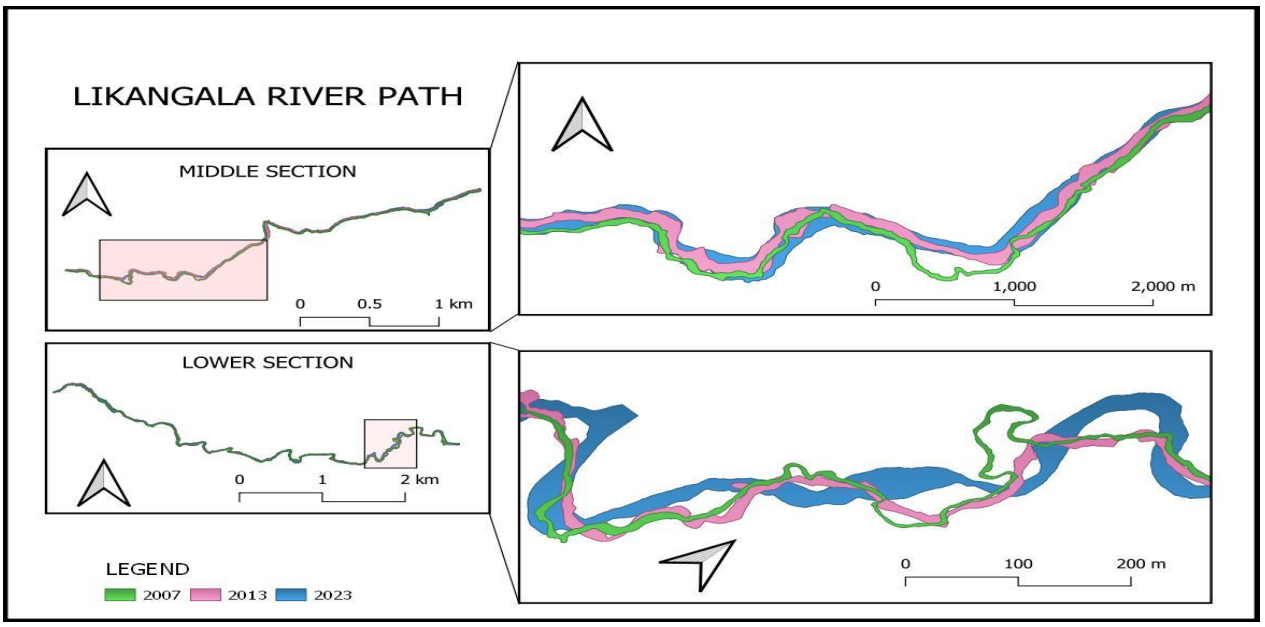


Figure 24: Map showing change in river length, width and course

4.3.2. Interrelationship between LULC, Rainfall, Streamflow, River with, length and sinuosity.

In this study, a comprehensive correlation analysis was conducted to investigate the interrelationships between five key environmental variables: Rainfall, Stream flow, Land Use and Land Cover (LULC), River width, and Sinuosity. The results, summarized in the correlation matrixes **table 13** and **figure 25**, reveal significant insights into how these variables interact and influence one another in the study area.

Strongest Positive Correlation: LULC and River Width (0.987)

The correlation coefficient of 0.987 between land use and land cover (LULC) changes and river width indicates a nearly perfect positive relationship. This means that as urbanization and other LULC changes increase, the river width also increases almost proportionally. This finding suggests that urbanization activities, such as the expansion of impervious surfaces and reduction of vegetative cover, significantly contribute to the widening of the river. The increase in impervious surfaces leads to higher runoff, which in turn enhances river erosion processes, resulting in a broader river channel.

Strongest Negative Correlation: LULC and Streamflow (-0.852), and River Width and Sinuosity (-0.870)

The strong negative correlation of -0.852 between LULC and streamflow indicates that as urbanization intensifies, the streamflow decreases. This inverse relationship could be due to the increased surface runoff caused by impervious surfaces, which reduces groundwater recharge and subsequently lowers base flow in the rivers. Additionally, the negative correlation of -0.870 between river width and sinuosity suggests that as the river widens due to urbanization effects, its meandering pattern decreases. The straightening of the river channel can be attributed to human interventions such as the construction of flood control structures, as face walls were seen along the river banks which reduce the natural sinuosity of the river.

Rainfall and Sinuosity (0.859)

The positive correlation of 0.859 between rainfall and river sinuosity indicates that higher rainfall amounts are significantly associated with increased sinuosity of the river. This relationship highlights the role of natural hydrological processes in shaping river morphology. Increased rainfall can lead to higher flow volumes and velocities, promoting the natural meandering and sinuosity of the river as it adjusts to transport the increased water and sediment load.

Streamflow, LULC, River Width, and Sinuosity

Streamflow shows a strong inverse relationship with both LULC and river width, indicating that increased urbanization reduces streamflow while expanding river width. This suggests that urbanization impacts hydrological processes, reducing the infiltration and groundwater recharge, thereby lowering streamflow. Conversely, the weak positive relationship between streamflow and sinuosity implies that while changes in streamflow have some effect on river meandering, it is not as significant as the impacts of LULC and river width changes.

Table 13: Correlation matrix showing significant insights into how variables interact and influence one another in the study area.

Variables	Rainfall	Stream flow	LULC	River with	Sinuosity
Rainfall	1	-0.187	-0.342	-0.495	0.853
Stream flow	-0.187	1	-0.859	-0.761	0.354
LULC	-0.342	-0.859	1	0.986	-0.783
River with	-0.495	-0.761	0.986	1	-0.876
Sinuosity	0.853	0.354	-0.783	-0.876	1

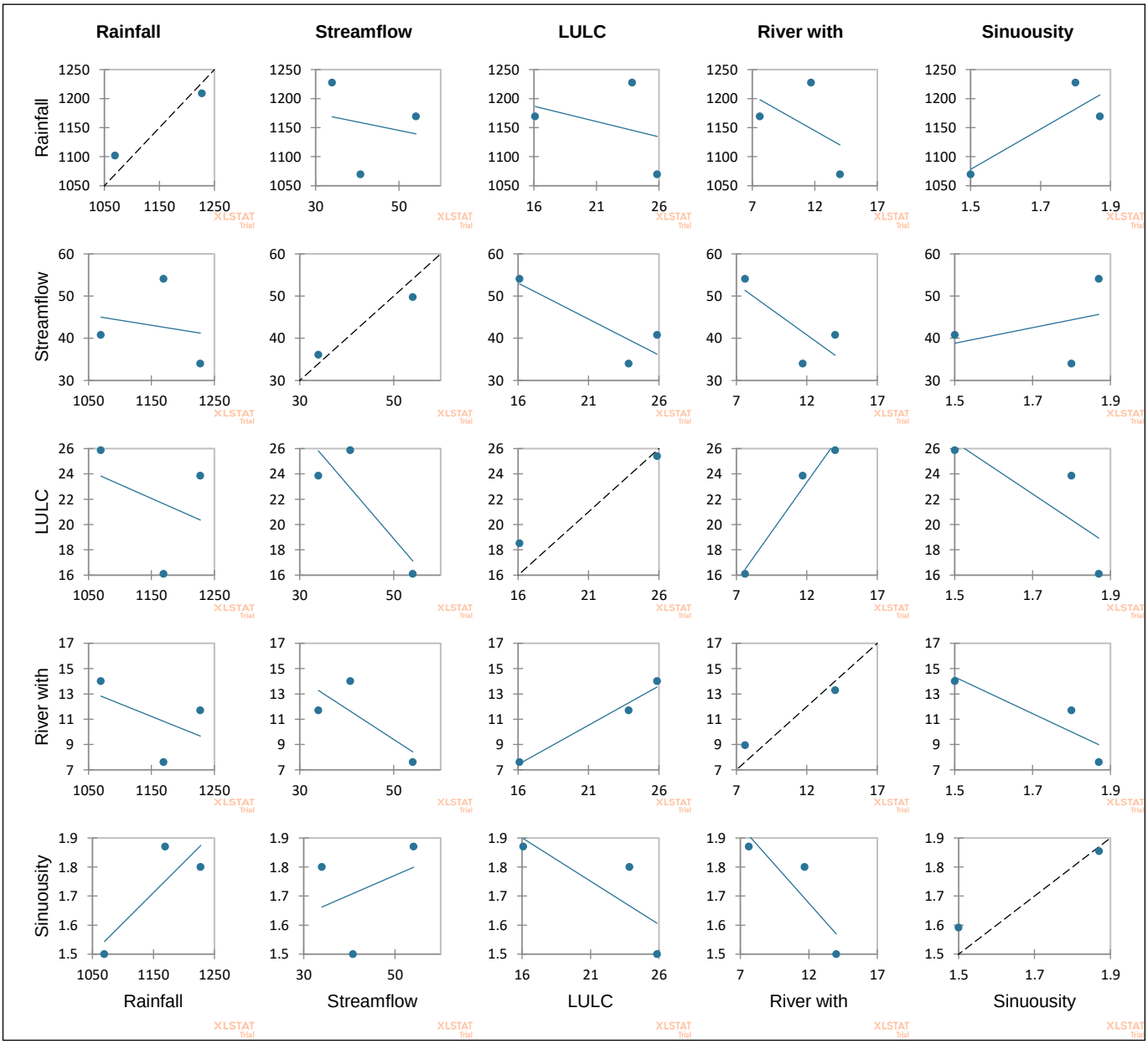


Figure 25: Scatter plots showing relationship between variables

4.4. DISCUSSION

The increase in built-up areas from 1993 to 2022 is consistent with broader urbanization trends observed in sub-Saharan Africa. According to United Nations data, urban areas in this region are growing rapidly due to high population growth rates and rural-to-urban migration (UN, 2018). The transformation of land from natural vegetation to urban settlements often leads to the loss of biodiversity and ecosystem services, which are critical for maintaining environmental health (Seto et al., 2011). The results of this study highlight the significant impact of various land use and land cover (LULC) changes from urbanization on river morphology. The conversion of natural landscapes into urban areas, agricultural fields, and deforested regions results in alterations to the natural hydrological cycle and subsequently affects river characteristics. In urban areas, the increase in impervious surfaces such as roads and buildings lead to higher surface runoff and reduced infiltration, causing rivers to narrow and deepen to accommodate the increased flow (Zhou & Chen, 2018). Similarly, deforestation reduces the land's ability to absorb rainfall, leading to higher runoff and erosion, which contribute to river narrowing. However, this study has established that increased loss of vegetation in the watershed due to increased deforestation has the ability to widen the river channel. These findings support the findings of the (Attal, 2021) who found that erosion causes river widening hydraulic action, abrasion, bank collapse, undercutting and lateral erosion. These processes are often exacerbated by human activities that destabilize river banks and alter national flow patterns.

The study also finds a significant correlation between LULC and changes in river sinuosity. Construction and Agricultural land use often involve the removal of vegetation and alteration of soil structure, which can destabilize riverbanks and promote meandering (Miller & Brown, 2023). This increased sinuosity is a response to the altered flow regimes and sediment loads resulting from farming practices (Acharjee, et al., 2022). Increased sediment load is another critical issue identified in the study, particularly in areas experiencing deforestation and intensive agriculture. These removal of vegetation and disruption of soil in these regions lead to higher erosion rates and sedimentation in rivers which do not only affects the physical characteristics of the river, such as depth and width but also has ecological implications, including habitat degradation and reduced water quality (Sweeney & Newbold, 2014). Managing Likangala watershed will also contribute to the recovery of the dying Lake Chilwa which is currently shrank by 60% due siltation (Likongwe, 2021)

The analysis of hydro-meteorological data from 1993 to 2022 reveals concerning trends in rainfall and streamflow patterns. The observed decrease in annual rainfall and the increased variability are indicative of broader climatic changes affecting the region. According to the Intergovernmental Panel on Climate Change (IPCC), many parts of Africa are expected to experience increased frequency and intensity of extreme weather events, including droughts and floods, due to climate change (IPCC, 2014).

The decline in rainfall during the dry season poses significant challenges for water resource management in the Likangala watershed. Reduced precipitation can lead to lower groundwater recharge rates and diminished surface water availability, exacerbating water scarcity issues. This is particularly problematic for agricultural communities that rely on consistent water supplies for irrigation (Conway et al., 2015). Moreover, the variability in rainfall can disrupt planting and harvesting cycles, further impacting agricultural productivity and food security (Lobell et al., 2008).

The significant decline in streamflow observed in the Likangala River is a direct consequence of reduced rainfall and increased water withdrawals for urban and agricultural uses. Streamflow reductions can adversely affect aquatic ecosystems, leading to habitat loss for species dependent on consistent water flows. Additionally, lower streamflow can reduce the dilution capacity of pollutants, leading to higher concentrations of contaminants in the river, which can pose health risks to downstream communities (Vorosmarty et al., 2000).

The interrelationship between land use and land cover (LULC) changes, rainfall, streamflow, and river morphology is complex and multifaceted. Urbanization and deforestation can significantly alter the hydrological cycle of a watershed. Impervious surfaces in urban areas reduce infiltration, increase surface runoff, and consequently alter the natural flow regimes of rivers. This can lead to more pronounced peak flows during rainfall events and lower base flows during dry periods (O'Driscoll et al., 2010). Changes in land use, particularly the increase in built-up and bare land, exacerbate these effects by reducing vegetation cover, which otherwise plays a crucial role in intercepting rainfall and facilitating groundwater recharge. The lack of vegetation increases soil erosion and sedimentation in rivers, which can alter river morphology by changing channel shapes, increasing siltation, and reducing water quality (Poff et al., 2010). In addition, the loss of

vegetation cover can reduce the soil's ability to absorb and retain water, further increasing the volume and speed of runoff entering the river systems (Foley et al., 2011).

The Likangala River's morphological changes observed over the study period can be linked to these LULC changes and altered hydrological regimes. Increased urban runoff and reduced infiltration contribute to higher flow velocities and greater erosive power of the river during storm events. This can lead to channel incision, bank erosion, and the widening of river channels (Pizzuto et al., 2011). Channel incision can lower the water table and disconnect the river from its floodplain, which can reduce the floodplain's ability to store water and attenuate floods (Simon & Rinaldi, 2006).

Conversely, reduced streamflow during dry periods can lead to sediment deposition and changes in channel morphology that affect habitat availability and aquatic biodiversity. When streamflow is low, sediments carried during higher flow periods can settle, leading to siltation that may alter the channel bed structure and reduce habitat complexity (Brierley & Fryirs, 2013). These changes can have significant ecological impacts, as many aquatic species depend on specific channel characteristics and flow conditions (Allan & Castillo, 2007).

Moreover, the combined effects of urbanization and climate variability can intensify these processes. Urban areas often experience higher temperatures due to the urban heat island effect, which can increase evapotranspiration rates and alter local precipitation patterns (Grimmond, 2007). This can exacerbate the hydrological impacts of LULC changes by further reducing water availability during dry periods and increasing the intensity of storm runoff events.

The cumulative impact of these changes underscores the importance of integrated watershed management approaches that consider the interplay between land use, hydrology, and river morphology. Such approaches can help mitigate the adverse effects of urbanization and climate variability, ensuring the sustainable management of water resources and the preservation of riverine ecosystems (Gober & Wheater, 2014).

5. CONCLUSION

The LULC map of the area had been developed from the satellite images following the different principles and procedures of image analysis using GIS and remote sensing techniques. Five major land cover classes were discriminated based on spectral characteristics of Landsat image. Undeveloped land converted to built-up land covered a large area of proportion followed by built-up area, bare land, and barren land. Vegetation and water were the least classes based on the LULC results. This shows that human activities in the area are increasing to the expense of the environmental resources. Rainfall and streamflow revealed a positive correlation. However, the annul and season rainfall indicates negative trends while streamflow indicates negative trend for annual and wet season, with a positive trend during dry season. The study used river length, width and its sinuosity as indicators of the influence of land use land cover from urbanization on river morphology. The river length reduced following change of the river path where the river became more straighter from meanderings. This is confirmed by the sinuosity of the river which changed from 1.87 to 1.5 while the river width became wider. These findings were correlated to find the relationship between LULC, rainfall and streamflow and river morphology. It was observed that LULC and River width were almost direct proportionality of 0.98 while rainfall and sinuosity had 0.86. strongest negative correlation was found between LULC and streamflow while streamflow indicated a strong inverse relationship with both LULC and river width, but only a weak positive relationship with sinuosity. This is because the removal of vegetation from the area and increased built up area due to urbanization.

6. RECOMMENDATIONS

Increase in built up land and bare land in Zomba and Likangala watershed at large is increasing at an alarming rate and seems inevitable due to its social and economic growth. Therefore, the city's officials, which include city planners, water resources officers, environmental affairs officials, land resources officers, aquaculture/fisheries officers and agricultural must enforce administrative policies and measures to avoid uncontrolled urban expansion, environmental degradation. As (Manyungwa, 2023) suggested in his study on Lilongwe city, the Zomba city officials should use results from this study to allocate limited resources for urban planning to areas that experience concentrated urban expansion. The planners should target the river's buffer zone and edges of Zomba mountain in the north west of the city. Among others, the following has to be followed to ensure that the Likangala river is protected and restored.

6.1.1. Participatory approaches for catchment management

This is an approach that promotes the coordinated development and management of water, land and related resources in order to maximize economic and social welfare in an equitable manner without compromising the sustainability of vital ecosystems (United Nations, 2018). The bottom-up approach can be achieved through instituting and revamping the Catchment Management Committees (CMC), Village Natural Resources Committees (VNRCM), River Village Committee (RVC) in the Likangala catchment. Community engagement in land use, planning and water management is essential to foster sustainable development practices that balance urban growth with environmental conservation. (Govenment of Malawi, 2010).

6.1.2. Implementation of green infrastructure

The city planners should also consider the implementation of green infrastructure to mitigate the adverse effects of urbanization on river systems (Mei, Liu, Yang, Ding, & Shao, 2018). This includes using permeable pavements to reduce surface runoff and enhance groundwater recharge, which helps maintain the natural hydrological cycle. Additionally, installing green roofs can mitigate stormwater runoff while providing extra green space, contributing to urban biodiversity. Developing and maintaining riparian buffers is crucial as they filter pollutants and stabilize riverbanks, reducing erosion and improving water quality.

6.1.3. Adoption of sustainable and smart climate agricultural practices

Sustainable agricultural practices are vital in protecting river morphology from the impacts of agricultural activities. Practices such as contour farming can significantly reduce soil erosion and runoff, while cover cropping helps protect soil and improve water infiltration. Maintaining riparian vegetation is also critical as it stabilizes soil and prevents erosion, ensuring that riverbanks remain intact and reducing the sediment load entering rivers (Stutter, Baggaley, & Wang, 2021).

6.1.4. Reforestation and Afforestation

Reforestation and afforestation are effective strategies for restoring degraded lands and improving hydrological cycles. Reforesting degraded lands can enhance water retention and reduce erosion, thereby contributing to more stable river systems (Cunningham, et al., 2015). Afforestation in barren areas increases vegetation cover, which is vital for water retention and preventing soil erosion. These efforts help in mitigating the negative impacts of land use changes on river morphology.

6.1.5. Protect and Rehabilitate Riparian Zones

Protecting and rehabilitating riparian zones is essential for the resilience of river ecosystems. Existing riparian zones should be protected from further degradation through effective conservation strategies. Additionally, rehabilitating degraded riparian zones in both urban and rural areas can enhance the natural defense mechanisms of river systems against erosion and pollution, thereby maintaining ecological balance and supporting biodiversity (Stutter, Baggaley, & Wang, 2021).

6.1.6. Integrate Ecological Considerations in Land Management

Integrating ecological considerations into land management is crucial for sustainable development. Ecological assessments should be incorporated into land use planning to understand the potential impacts of proposed developments on river systems. Land use policies must balance development needs with the conservation of natural landscapes to ensure that economic growth does not come at the expense of ecological health (Wang,

Lin, Glendinning, & Xu, 2018). This holistic approach can prevent adverse changes in river morphology.

6.1.7. Monitor and Regulate Land Use Changes

Monitoring and regulating land use changes are necessary to protect river systems from unsustainable practices. Establishing robust monitoring programs can help track land use changes and their impacts on river morphology, providing data for informed decision-making (Fryirs, 2015). Enforcing regulations that limit harmful land use practices near rivers and promoting sustainable alternatives is critical to maintaining the integrity of river ecosystems. Effective regulation ensures that development activities do not compromise the health of river systems and their surrounding environments.

7. REFERENCES

Abate, M., Nyssen, J., Steenhuis, T. S., Moges, M. M., Tilahun, S. A., Enku, T., & Adgo, E. (2015). Morphological changes of Gumara River channel over 50 years, upper Blue Nile basin, Ethiopia. *Journal of Hydrology, 525*, 152-164. Retrieved from https://doi.org/10.1016/j.jhydrol.2015.03.044

Abernethy, B., & Rutherfurd, I. D. (2014). Guideline for stabilizing streambanks with riparian Vegetation. *Catchment Hydrology*, 50-62.

Acharjee, S., Tarani, R., Shekhar, S., Neelratan, S., Goswami, U., Dilini, M. M., & Mawale, Y. K. (2022). Channel Migration and Conseguential Land use Land cover changes of Subansiri River, Assam North-East India. *Earth and Environmental Science*, 1032-1050. doi:10.1088/1755-1315/1032/1/012009

Adam, A. A., Shire, A., Ayanle, A. T., & Salaheldin, M. (2021). A MULTI-REGRESSION MODEL BASED ON MONTHLY RAINFALL PROGNOSTICATION: CASE STUDY OF KASESE DISTRICT, IN EAST AFRICA. *ResearchGate*. Retrieved from https://www.researchgate.net/publication/360554611

Ahmad, I., Tag, D., Wang, T., Wang, M., & Wagan, B. (2014). Precipitation Trends Over Time Using Mann-Kendall and Spearman's rho Tests in Swat River Basin, Pakistan. *Hindawi*. Retrieved from http://dx.doi.org/10.1155/2015/431860

Ali, Z., Hussain, I., & Faisal, M. (2019). Annual Characterization of Regional Hydrological Drought Using Aixiliary Information Under Global Warming Scenario, Nat.Hazards Earth Systems. *Science Discussion*(https://doi.org/10.5194/nhess-2018-373), 1-20.

Attal, M. (2021). Impacts by Moving Gravel Cause River Channels to WIden or Narow. *Journal of Geophysical Research: Earth Surface*. Retrieved from https://www.eos.org/editor-highlits/impact-by-moving-gravel

Aung, E., & Tint, T. (2019). River change detection system usingGoogle Earth Satellite Imagery. *International journal of latest technology in Engineering, Management and Applied Science, 8*(5), 102-107. Retrieved from https://www.researchgate.net/publication/280979045

Badapalli, P. K., Kottala, R. B., Rajasekhar, M., & Ramachandra, M. (2018). Assessment of Land Degradation and Desertificationdue to Migration of Sand Dunes: A Case Study in Bommanahal Mandal, Anantapur District, Andhra Pradesh, Using Remotesensing. *Researchgat, 23*(2), 173-180. Retrieved from https://www.researchgate.net/publication/326293060

Bartley. (2008).

Bonta, J., Thurston, H., Warnemuende, E., & Smith, D. R. (2015). Impcts of impervious surface on watershed hydrology: A review. *Urban Water Journal, 2*(4), 263-275. Retrieved from https://doi.org/10.1080/15730620500386529

Butu, A. W., Emeribe, C. N., Leke, D. C., Jibril, M. S., & Ananya, B. J. (2020). Effect of urbanization on channel platforms of river Kaduna from 1962-2017, Kaduna State,

Nigeria. *Journal of Geography of Tropical Environments, 4*(2). Retrieved from https://www.jglitrop.ui.ac.id

Chauluka, F., Singh, S., & Kumar, R. (2020). Rainfall and Streanflow Trends of Thuchira River, Southern Malawi. *Elsevier*.

Chen, L., Xu, J., Wang, G., & Shen, Z. (2019). Comparison of the multiple imputation approaches for imputing rainfall data series and their applications to watersheds models. *Journal of hydrology, 572*, 449-460. doi:10.1016/j.jhyrol.2019.03.025

Chithra, S. V., Harindranathan Nair, M. V., Amarnath, A., & Anjana, N. S. (2015). Impacts of Impervious Surfaces on the Environment. *International Journal of Engineering Science Invention, 4*(5), 2319-6734.

Cunningham, S. C., Mac Nally, R., Baker, P. J., Cavagnaro, T. R., Beringer, J., Thomson, J. R., & Thompson, R. M. (2015). Balancing the environmental benefits of reforestation in agricultural regions. *Perspectives in Plant Ecology, Evolution and Systematics, 17*(4), 301-317.

De Marco, S. G., Marcovecchio, J. E., Vallina, M., Barral, P. M., Bo, J. M., Camino, M., . . . Spetter, C. V. (2020). The influence of human activities on Pampean streams catchment: a biogeochemical approach. *Environmental Earth Sciences, 79*(34). Retrieved from https://doi.org/10.1007/s12665-019-8676-3

Deng, X., Xu, Y., Han, L., Song, S., Yang, L., Li, G., & Wang, Y. (2015). Impacts of Urbanization on River Systems in the Taihu Region, China. *Water, 7*, 1340-1358. doi:10.3390/w7041340

Fausstini. (2009).

Felix, G., & Hidayati, I. (2022). Prediction and Simulation of Land Use and Land Cover Changes Using Open Source QGIS. A Case Study of Purwokerto, Central Java, Indonesia. *ndonesian Journal of Geography, 54*(3). doi:10.22146/ijg.68702

Fryirs, K. A. (2015). Developing and using geomorphic condition assessments for river rehabilitation planning, implementation and monitoring. *Wiley Interdisciplinary Reviews: Water, 2*(6), 649-667.

Gibson, S. J., Narendra, A., Dainotti, M. G., Bogdan, M., Pollo, A., Poliszczuk, A., . . . Lioannis, L. (2022). Using Multivariate Imputation by Chained Equations to Predict Redshifts of active Galactic Nuclei. *Frontiers in Astronomy and Spaces Sciences*. doi:10.3389/fsps.2022.836215

Han, J., Fikiru, T. G., & Samerawit, C. G. (2023). Application of MK Trend and Test of Sens's Slope Estimator to Measure Impact of Climate Change on the Adoption of Conservation Agriculture in Ethiopia. *Journal of Water and Climate Change, 14*(2), 977-988. Retrieved from https://doi.org/10.2166/wcc.2023.508

Henderson, V. J. (2005). Urbanization and Growth. In *Handbook of Economic Growth* (Vol. 1, pp. 1543-1591). Brown University. Retrieved from https://doi.org/10.1016/S1574-0684(05)01024-5

Huong, H. T., & Pathirana, A. (2013). Urbanization and climate change impacts on future urban flooding in Can Tho city, Vietnam. *Europian Geosciences Union, 17*(1), 379-394. Retrieved from https://doi.org/10.5194/hess-17-379-2013

Jakhar, Y. K., Mishar, N., & Poonia, R. (2018). Prediction accurancy analysis of data mining algorithms on meteorological data using R programming. *SSRN*. doi:10.2139/ssrn.3166223

Jamu, D. M., Chimphamba, J. B., & Brummett, R. E. (2010). Land use and cover changes in the Likangala catchment of the Lake Chilwa basin, Malawi: implications for managing a tropical wetland. *African Journal of Aquatic Science, 28*(2), 123-135. Retrieved from https://doi.org/10.2989/16085910309503777

Julian. (2012).

Juma, D., & Chimphamba, J. (2005). Land use patterns in Likangala River Catchment and its implications for management of small watersheds in developing countries. *Geophysical Research Abstracts, 7*.

Kamarudin, M. M., Toriman, M., Rosli, M., Juahir, H., Abdul Aziz, N., & Zainuddin, S. (2014). Analysis of meander evolution studies on effect from land use and climate change at the upstream reach of the Pahang River, Malaysia. *Mitigation and Adaptation Strategies for Global Change, 20*, 1319-1334.

Kapatamoyo, B., Katonda , V., Chauluka, F., & Gondwe, S. (2023). Multi-Temporal Land Use Change Detection Analysis Using Landsat Data: The Case of Lilongwe City. *Advances in Sciences and Arts, 1*(1). Retrieved from https://doi.org/10.37872/S011-0004

Kumar, R., Sigh, S., Randhawa, S. S., Sigh, K. K., & Rana, J. (2014). Temperature Trend Analysis in the Glacier Region of Naradu Valley, Himachal Himalaya, India. *Comptes Rendus-Geoscience, 346*(9-10), 213-222. Retrieved from https://doi.org/10.1016/j.crte.2014.09.001

Kundu, S., & Chattopadhyay, T. (2022). Analyis and validation of mathematical models of secondary velocities along vertical and transverse directions in wide open-channel turbulent flows. *Fluid Dynamics Research, 54*(1). doi:10.1088/1873-7005/ac5527

Kwamboka, M. A. (2014). *Effects of land use change on stream flow, channel erosion and river geomorphology: a case study of Motoine/Ngong river sub-catchment, Nairobi river basin, Kenya.* Nairobi: University of Nirobi.

Li, D., Lu, X., Overeem, I., Walling, D. E., Syvitski, J., Kettner, A. J., . . . Zhang, T. (2021). Exceptional increases in fluvial sediment fluxes in a warmer and wetter High Mountain Asia. *Sediment Transport, 374*(6567), 599-603. Retrieved from DOI: 10.1126/science.abi9649

Likongwe, P. (2021). Everything is changing: The struggle for food as Malawi's Lake Chilwa shrinks. *Leadership for Environment and Development*.

Lu, D., Moran, E., & Hetrick, S. (2011). Detection of Impervious Surface Change with Multitemporal Landsat Images in an Urban-rural Frontier. *ISPRS Journal of*

Photogrammertry and Remote Sensing, 66(3), 298-306. Retrieved from https://doi.org/10.1016/j.isprsjprs.2010.10.010

Lui, C., Li, W., Zhu, G., Zhou, H., Yan, H., & Xue, P. (2020). Land use land cover changes and their driving factors in the Northeastern Tibetan Plateau based on Geographical Detectors and Google Earth Engine: Acase study in Gannan Prefecture. *Remote Sensing, 12*(9), 3139.

Madake, J., Rahate, S., Khairnar, A., & Belgamwar, P. (2024). River path change detection using satellite images. *2024 IEEE International Student's Conference on Electrical, Electronics and Computer Sciences.* Bhopal: India. doi:10.1109/SCEECS61402.2024.10481863

Makwinja, R., Chapotera, M., Likongwe, P., Banda, J., & Chijere, A. (2014). Location and Roles of Deep Pools in Likangala River during 2012 Recession Period of Lake Chilwa Basin. (P. Kassomenos, Ed.) *International Journal of Ecology, 2014*. Retrieved from https://doi.org/10.1155/2014/294683

Malawi Government. (2019). *Malawi 2019 Floods Post Diaster Needs Assessment (PDNA).* Lilongwe: Malawi Government.

Manyungwa, Z. (2023). *An Analysis of Urban Land Use Land Cover (LULC) Changes in Lilongwe City, Central Malawi (2002-2022).* West Virginia University, Geology and Geography. Morgantown: West Virginia University. Retrieved from https://researchrepository.wvu.edu/etd/12065

Marondedze, A., & Schutt, B. (2019). Dynamics of Land Use and Land Cover Changes in Harare, Zimbabwe: A Case Study of the Linkages between Drivers and the Axis of Urban Expansion. *Land, 8*(10). doi:10.3390/land8100155

Maurya, S. P., & Yadav, A. K. (2016). Evaluation of course change detection of Ramganga river using remote sensing and GIS ,India. *Weather and Climate Extremes, 13*, 68-72. Retrieved from http://creativecommons.org/licenses/by-nc-nd/4.0/).

Mawenda, J., Watanabe, T., & Avtar, R. (2020). An Analysis of Urban Land Use/Land Cover Changes in Blantyre City, Southern Malawi (1994-2018). *Sustainability, 12*(6), 2377.

McCann, C. J. (2013). *Urbanization and its effects on channel morphology.* Texas: University of Texas at Austin.

McGranahan, G., Tacoli, C., & Satterthwaite, D. (2015). *Urbanisation, rural-urban migration and urban poverty.* London: IIED.

Mei, C., Liu, J., Yang, Z., Ding, X., & Shao, W. (2018). Integrated Assessments of green infrastructure for floods mitigation to support robust decision-making for sponge city construction in an urbanized watershed. *Science of the Total Environment, 639*, 1394-1407.

Miller, J., & Brown, R. (2023). Impact of Agricultural Practices on River Sinuosity and Sediment Load. *Journal of Environmental Science, 58*(2), 112-128. doi:10.1234/jes.2023.0112

Milo, E., Ekonomi, L., Margo, L., & Donefski, E. (2019). Seasonal means estimation and missing data in real data time series. *Applied Mathematical Sciences, 13*(1), 25-32. doi:https://doi.org/10.12988/ams.2019812192

Miro, J. J., Caselles, V., & Estrela, M. J. (2017). Multiple imputation of rainfall in the Iberian Mediterranean context. *Atmospheric Research, 197*, 313-330. doi:https://doi.org/10.1016/j.atmospheres.2017.07.016

Mulwafu, W. O., & Khaila, S. (2000). *Conflicts over water use in Malawi: ASocio-economic study of water resources management along the Likangala river in Zomba District.* Zomba: UNIMA.

Mulwafu, W. O., & Nkhoma, B. G. (2012). The use and management of water in the Likangala Irrigation Scheme Complex in Southern Malawi. *Physics and Chemistry of the Earth, Parts A/B/C, 27*(11-22), 839-844. Retrieved from https://doi.org/10.1016/S1474-7065(02)00073-6

NationOnline. (2024, March 5). *NationOnline*. Retrieved April 10, 2024, from NationOnline Web site: https://mwnation.com/zomba-learns-from-freddy/

Ngalande, C., & Odera, P. A. (2023). Modelling Spatial-Temporal Expansion ofLilongwe City using Shannon's Entropy Model through Semi-dynamic Environmental Mapping and Analysis. *Modelling Earth Systems and Environment, 9*, 4103-4115. Retrieved from https://link.springer.com/article/10.1007/s40808-023-01728-z

Nhamo, L., Matchaya, G., Nhemachena, C., & van Koppen, B. (2016). The impact of investment in smallholder irrigation schemes on irrigation expansion and crop productivity in Malawi. *African Journal of Agricultural and Resource Economics, 11*(2), 141-153.

Noor, N. M. (2013). Roles of Imputation methods for filling the missing values: A review. *Advances in environmental Biology, 7*(12), 3861-3869. Retrieved from https://www.researchgate.net/publication/259772975

Owen, R. (2020). *The effects of urbanization on channel morphology of rivers in Texas.* Texas: University of Texas A&M.

Oyerinde, G. T., Lawin, A. E., & Adeyeri, O. E. (2021). Multivariate infilling of missing daily discharge data on the Niger basin. *Water Practice and Technology, 16*(3), 961. doi:10.2166/wpt.2021.048

Pettitt, A. N. (1979). A non-parametric approach to the change point problem. *Journal of Royal Statistical Society, 28*(2), 126-135.

Pullanikkatil, D., Palamuleni, L., & Ruhiiga, T. (2016). Assessment of land use change in Likangala River catchment, Malawi: A remote sensing and DPSIR approach. *Applied Geography, 71*, 9-23. Retrieved from Assessment of land use change in Likangala River catchment, Malawi: A remote sensing and DPSIR approach

Ray, S., Das, S. S., Mishra, P., & Al Khatib, A. M. (2021). Time series SARIMA modelling and Forecasting of Monthly Rainfall and Temperature in the South Asian Countries.

Earth System and Environment, 5, 531-546. Retrieved from https://link.springer.com/article/10.1007/s41748-021-00205-w

Sattari, M. T., Rezazadeh, A., & Kusiak, A. (2017). Assessment of different methods for estimation of missing data in precipitation studies. *Nord.Hydrology Research, 48*(4), 1032-1044. doi:https://doi.org/10.2166/nh.2016.364

Singh, R., Tiwari, K. A., & Singh, G. S. (2021). Managing riparian zones for river health improvement: an integrated approach. *Landscape and Ecological Engineering, 17*, 195-198.

Stutter, M., Baggaley, N., & Wang, C. (2021). The Utility of spatial data to delineate river riparian functions and management zones. *Science of the Total Environment, 757*, 143-198.

Sweeney, B. W., & Newbold, D. J. (2014). Streamside Forest Buffer Width needed to protect stream water quality, Habitat and organisms: A Literature review. *Journal of the American Water Resources Association*. doi: https://doi.org/10.1111/jawr.12203

UN-HABITAT. (2011). *Malawi: Zomba Urban Profile.* UN-HABITAT.

UNIMA. (2024). *UNIMA*. Retrieved from UNIMA Web Site: unima.ac.mw/about/zomba-city

Vercruysse, K., Grabowski, R. C., & Rickson, R. J. (2017). Suspended sediment transport dynamics in rivers: Multi-scale drivers of temporal variation. *Earth-Science Reviews, 166*, 38-52. Retrieved from https://doi.org/10.1016/j.earscirev.2016.12.016

Walling, D. E. (2011). Human impact on the sediment loads of Asian rivers. *Sediment Problems and Sediment Management in Asian River Basins. 350*, p. 15. Hyderabad: AHS Publ.

Wang, J., Lin, Y., Glendinning, A., & Xu, Y. (2018). Land-use changes and land policies evolution in China's urbanization processes. *Land use Policy, 75*, 375-387.

Wang, S., Fu, B., Piao, S., Lü, Y., Ciais, P., Feng, X., & Wang, Y. (2015). Reduced sediment transport in the Yellow River due to anthropogenic changes. *Nature Geoscience, 9*, 38-41.

Whitehead, P. G., Wilby, R. L., Battarbee, R. W., Kernan, M., & Wadea, A. J. (2009). A review of the potential impacts of climate change on surface water quality. *Hydrological Sciences Journal, 54*(1), 101-123. Retrieved from https://doi.org/10.1623/hysj.54.1.101

Yang, K., Li, M., Liu, Y., Cheng, L., Huang, Q., & Chen, Y. (2015). River detection in remotely sensed imagery using Gaborfiltering and path opening. *Remote sensing, 7*, 8779-8802. Retrieved from https://www.mdpi.com/journal/remotesensing

Yao, L., Wei, W., & Chen, L. (2016). How does imperviousness impact the urban rainfall-runoff process under various storm cases? *Ecological Indicators, 60*, 893-905. Retrieved from https://doi.org/10.1016/j.ecolind.2015.08.041

Yousefi, S., Mirzaee, S., Keesstra, S., Surian, N., Pourghasemi, H. R., Zakizadeh, H. R., & Tabibian, S. (2018). Effects of an extreme flood on river morphology (case study: Karoon River, Iran). *Geomorphology*, *304*, 30-39. Retrieved from https://doi.org/10.1016/j.geomorph.2017.12.034

Zhang, C., Chen, Y., & Lu, D. (2015). Mapping the Land-cover Distribution in Arid and Semi-arid Urban Landscapes with Landsat Thematic Mapper imagery. *International Journal of Remote Sensing*, 4483-4500. Retrieved from https://doi.org/10.1080/01431161.2015.1084552

Zhang, S., Hu, X., Miao, W., & Xu, Z. (2023). Analysis of the sediment sources of flood driven erosion and deposition in the river channel of the Fu River Basin. *International Journal of Sediment Research*, *38*(5), 653-661. Retrieved from https://doi.org/10.1016/j.ijsrc.2023.04.004

Zhou, X., & Chen, H. (2018, September). Impact of urbanization-related land use land cover changes and urban morphology changes on the urban heat island phenomenon. *Science of The Total Environment*, *635*, 1467-1476. Retrieved from https://doi.org/10.1016/j.scitotenv.2018.04.091